M.FENDAL

PERFORMANCE EVALUATION OF A SINGLE CYLINDER HBO ENGINE

THE GRADUATE SCHOOL OF NATURAL AND APPLIED SCIENCES
OF
ATILIM UNIVERSITY

METİN FENDAL

A MASTER OF SCIENCE
THESIS
IN
THE DEPARTMENT OF MANUFACTURING ENGINEERING

JAN 2020

ATILIM UNIVERSITY 2020

PERFORMANCE EVALUATION OF A SINGLE CYLINDER HBO ENGINE

A THESIS SUBMITTED TO
THE GRADUATE SCHOOL OF NATURAL AND APPLIED SCIENCES
OF
ATILIM UNIVERSITY

BY

METİN FENDAL

IN PARTIAL FULFILLMENT OF THE REQUIREMENTS
FOR
THE DEGREE OF MASTER OF SCIENCE
IN
THE DEPARTMENT OF MANUFACTURING

JAN 2020

Approval of the Graduate School of Natural and Applied Sciences, Atilim University.

_____

Prof. Dr. Ali Kara
Director

I certify that this thesis satisfies all the requirements as a thesis for the degree of **Master of Science in Manufacturing Engineering, Atilim University**.

_____

Prof. Dr. Engin Kılıç
Head of Department

This is to certify that we have read the thesis PERFORMANCE EVALUATION OF A SINGLE CYLINDER HBO ENGINE submitted by Metin FENDAL and that in our opinion it is fully adequate, in scope and quality, as a thesis for the degree of Master of Science.

_____	_____
Prof. Dr. Demir Bayka Co-Supervisor	Asst. Prof. Dr. Rahim Jafari Supervisor

Prof. Dr. Engin Kılıç
Manufacturing Engineering, Atılım University _____

Dr. Rahim Jafari
Automotive Engineering, Atılım University _____

Prof. Dr. Demir Bayka
Mechanical Engineering, Başkent University _____

Dr. Ramin Barzegar
Automotive Engineering, Atılım University _____

Dr. Kutluk Bilge Arıkan
Committee Member, TED University _____

Date: *21.01.2020*

I hereby declare that all information in this document has been obtained and presented in accordance with academic rules and ethical conduct. I also declare that, as required by these rules and conduct, I have fully cited and referenced all material and results that are not original to this work.

Name, Last Name : Metin FENDAL

Signature :

ABSTRACT

PERFORMANCE EVALUATION OF A SINGLE CYLINDER HBO ENGINE

Fendal, Metin

Degree of Master, Department of Manufacturing Engineering

Supervisor : Dr. Rahim Jafari

Co-Supervisor : Prof. Dr. Demir Bayka

January 2020, 70 pages

The development of 2 and 4 stroke cycle prototype spark ignition engines using gasoline, manufactured by Minisan A.Ş., is intended in this study. The engines, designed to operate with carburetors and conventional ignition system, functioned successfully. The first designed engine was manufactured with a similar cylinder head, valve configuration, spark plug location and equal cylinder diameter and piston stroke with the ACME model engine, for comparison. The geometry of the connecting rod was altered. The center of the crankshaft shifted approximately 40 – 70 mm from the center of the cylinder. The specific fuel consumption of the new engine was lower and a decision was made to develop it. After the first 340 cc prototype, 2 cylinder, air and water cooled prototype engines were manufactured. A 340 cc engine was also developed within the scope of this thesis. Appropriate combustion chamber geometry and valve configuration for the thermodynamic cycle of these engines were not included in this study. Within the scope of the thesis, commercial electronic fuel injection and ignition systems were acquired and adapted to the engines. These systems were operated by electronic control units (ECU) which were acquired. Theoretical simulation and experimental performance and mapping work were done on the engines for programming the ECU. Two dimensional tables were constructed for the injectors and igniton systems to follow according to the working modes of the engines and were uploaded to the ECU's. Performance tests were conducted with the

upgraded electronic injection and ignition system of the engines. In comparison to the operation of the engines with carburetors and conventional ignition system, for same engine speed ranges and loads up to 20 percent increase was observed for the excess air coefficient and up to 30 percent decrease was observed for the brake specific fuel consumption.

Keywords: Internal combustion engine, ignition system, performance evaluation tests.

ÖZ

TEK SİLİNDİRLİ HBO MOTORUNUN PERFORMANS GELİŞİMİ

Fendal, Metin
Yüksek Lisans, Mühendislik Bölümü
Tez Yöneticisi : Dr. Rahim Jafari
Ortak Tez Yöneticisi : Prof. Dr. Demir Bayka

Ocak 2020, 70 sayfa

Bu tezde Minisan A.Ş. tarafından prototipleri üretilen, tek ve iki silindirli, 2 ve 4 zamanlı, buji ateşlemeli, benzinle çalışan içten yanmalı motorların geliştirilmesi ve performanslarının deneylerle saptanması amaçlandı. Karbüratörlü ve konvansiyonel ateşlemeli olarak tasarlanan motorlar başarılı bir şekilde çalıştı. İlk tasarlanan motorla benzer silindir kafası, sübab düzeni, buji yerleşimi, aynı silindir çapı ve piston stroku ile üretildi. Sadece biyel kolunun geometrisi değiştirildi. Bununla birlikte krank milinin merkezi silindir merkezinden yaklaşık 40 – 70 mm kaydı. Benzer tork ve devirlerde yeni motorun özgül yakıt tüketiminin daha düşük olduğu görüldükten sonra geliştirilmesine karar verildi. 340 cc süpürme hacimli olan ilk prototipten sonra 2 silindirli hava ve su soğutmalı prototip HBO motorlar üretildi. Bu tez kapsamında 340 cc hacimli olan motorun da geliştirme çalışması yapıldı. Motorların çevrimlerine uygun yanma odası ve sübap ayarları için gereken kam mili geometrisi bu çalışmanın kapsamına dahil edilmedi. Tez kapsamında piyasadan temin edilen elektronik yakıt püskürtmeli ve elektronik ateşlemeli sistemler motorlara adapte edildi. Bu sistemler, satın alınan elektronik kontrol ünitelerinin (EKÜ) denetimi altında çalıştırıldı. Ekü programlaması için prototip motorlar üzerinde teorik simülasyon ve deneysel performans haritalama çalışmaları yapıldı. Enjektörlerin ve ateşleme sistemleri ile performans deneyleri yapıldı. Motorların karbüratörlü ve konvansiyonel ateşlemeli sistemleri ile performans deneyleri yapıldı. Motorların karbüratörlü ve konvansiyonel

ateşlemeli aynı devir aralığı ve yük aralığındaki çalışmalarına göre hava fazlalık katsayılarında %20’ e varan artış ve özgül yakıt tüketimlerinde %30’a varan azalma görüldü.

Anahtar Kelimeler: İçten yanmalı motor, motorun ateşleme sistemi, performans geliştirme testleri.

To my mother and my father who are always with me ...

ACKNOWLEDGMENTS

I would like to thank my supervisor Dr. Rahim Jafari for his guidance, advice and encouragements during the study.

I shall also thanks for helping me out with this thesis for Prof. Dr. Demir Bayka.

I would like to thank my master committee and jury members, Prof. Dr. Engin Kılıç, Dr. Ramin Barzegar, Dr. Kutluk Bilge Arıkan for their valuable suggestions and helpful comments on this study.

Furthermore, I thank the members of Atılım University.

Thank Hasan Basri Özdamar for giving us a chance to work with the engine.

The financial support of The Scientific and Technical Research Council of Turkey (TUBITAK) is also acknowledged.

TABLE OF CONTENTS

LIST OF TABLES

TABLES

LIST OF FIGURES

FIGURES

LIST OF SYMBOLS/ABBREVIATIONS

B	:	Cylinder Bore
p	:	Cylinder Pressure
a	:	Crank offset
A_p	:	The Area Of The Piston
F	:	Force
T	:	Torque
$_{pme}$	:	Mean Effective Pressure
V_d	:	Engine Displacement (Volume)
$_{nr}$	:	Number Of Crankshaft Rotations For A Complete Engine Cycle
P	:	Power
ω	:	Angular Velocity
W	:	Watt
$_{bhp}$	:	Brake Horse Power
$_{rpm}$	:	Rotations Per Minute
HP	:	Horse Power
$_{ma}$	:	Mass Of Air
$_{mf}$	:	Mass Of Fuel
V_f	:	Volume Of Fuel
V_t	:	The Total Volume Of An Engine
nc	:	The Total Number Of Cylinders
V_{cyl}	:	The Volume Of One Cylinder
V_d	:	The Displaced (swept) Volume
V_c	:	The Clearance Volume
IV	:	Intake Valve
EV	:	Exhaust Valve
TDC	:	Top Dead Center
BDC	:	Bottom Dead Center
S	:	Piston Stroke
r	:	Connecting Rod Length

a	:	Crank Radius (offset)
x	:	Distance Between The Crank Axis And The Piston Pin Axis
θ	:	Crank Angle
nv	:	The Volumetric Efficiency
V_a	:	Volume Of Intake Air
V_d	:	The Theoretical Volume Of The Engine/Cylinder
ρa	:	Air Density
N_e	:	Engine Speed
P_a	:	Air Pressure
T_a	:	Temperature
R_a	:	Gas Constant For Dry Air
HBO	:	Hasan Basri Özdamar Engine
LGA	:	Lombardi 340 Gasoline Engine
ECU	:	Electronic Control Unit
GDI	:	Gasoline Direct Injection
BME	:	Dynamometer Control Unit

CHAPTER 1

INTRODUCTION

1.1. General

The automotive industry in our country started in the late 1920's with the assembly plant of Ford Motor Company in Tophane, Istanbul. After the end of the World War II, private corporations, Jeep Company, in partnership with the American company Willys, established a production factory in Tuzla, Istanbul. In 1955 in the Çayırova district of Kocaeli, a truck assembly factory titled Federal Türk Kamyonlar A.Ş. was established. In 1956, the Minneapolis-Moline established Turkish Tractor and Agricultural Machinery assembly factory in Ankara. In 1959, Ford Motor Company and the Koç Group jointly established Otosan A.Ş. In 1962, in partnership with OYAK and International Harvester, the production of various vehicles started under the name of Turkish Automotive Industry (TOE). In 1963, the company titled Otobüs Karoseri A.Ş. started to produce Magirus busses with licensing. TUBITAK was established on the of July 17, 1963. As a result, TUBITAK-supported projects on automotive field started in our technical universities. In 1966, Otosan began manufacturing vehicles under the brand name of Anadol in Istanbul. This was followed with other vehicles such as Murat 124® by TOFAŞ A.Ş., established in Bursa in 1968 and Renault 12® which was produced by OYAK-Renault partnership.

Today, Turkey's automotive industry has reached an important place in the world market. It has the largest share in our exports business. Various Turkish designs are appreciated and preferred in foreign markets. However, the engines of most of these vehicles are still being imported. Original engine studies started with a small, single diesel engine at Pancar A.Ş. which is still in operation. In 1986, Ford Otosan designed the first diesel engine for automobiles with the brand name Erk and produced short-term series production. Following that, the four-cylinder Ford Puma diesel engine was developed to a five-cylinder version with the support of TUBITAK TEYDEB. This engine was appreciated in the United States of America and Otosan Connect

commercial vehicles continues to be in sale in the USA with exportation records. Otosan company has designed and produced 7, 9, 11- and 13-liter models of the Ecotorq® engine with TÜBİTAK supported projects in the Research and Development center established by Marmara Research Center in GEBZE. China has acquired the license of the 13-liter engine and started its mass production. This was the first exportation in Turkey in the field of automotive technology. TÜBİTAK's support to universities in the automotive sector continues to increase.

In this context, the internationally patented and prototyped HBO (Hasan Basri Özdamar) brand spark ignition single and multi-cylinder internal combustion engine invented by Minisan A.Ş. was studied at Atılım University Automotive Engineering Department. This thesis aims at describing the development studies of this engine and the obtained results [1].

The present invention relates to environmentally friendly and high-speed explosive internal combustion engines. In this engine, fuel is used with maximum efficiency through the development of the crank link mechanism and the least waste gas is released [2]. Since the invention of internal combustion engines by Otto, studies have been carried out on internal combustion engines aimed at providing high engine power and fuel savings by improving the crankshaft, connection path and piston mechanism. An internal combustion engine with a tuned crankshaft positioned at a predetermined distance from the vertical axis of the cylinder counter to the direction of rotation of the crankshaft (Figure 1.1 and Figure 1.2) was invented in order to achieve high performance and torque [2].

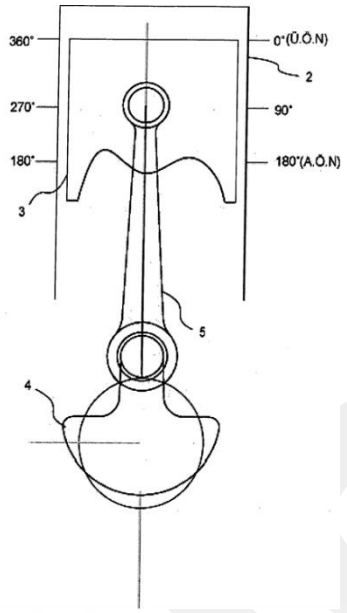

Figure 1.1: Front schematic view of the cylinder system of a traditional engine [2].

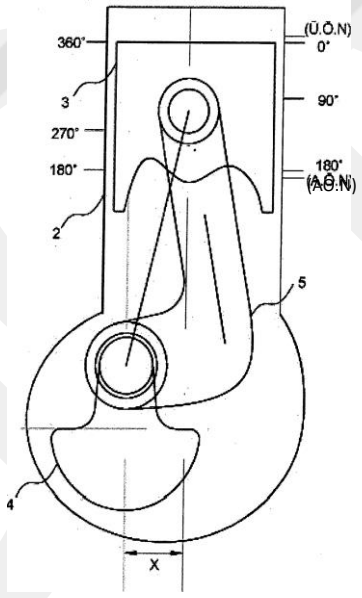

Figure 1.2: Schematic view of the position of the piston in the cylinder system of the engine that is the subject of the invention [2].

This engine is defined as having an offset crankshaft-connecting rod mechanism from the central axis of the cylinder and aims to increase the efficiency of the engine.

The engine is placed at a predetermined distance from the axis of the crank arm mechanism with the piston on top to rotate the crankshaft and the engine is turned off because a small moment arm improves its performance [2].

The geometry of the connecting rods of the HBO engine used in this study is different from the geometry of normal internal combustion engines. Due to this difference, the speed profile of the piston moving between the bottom dead center (BDC) and the top dead center (TDC) changes.

The Lombardini LGA engine is a single-cylinder, 340cc, spark ignition, 4-stroke, and air-cooled internal combustion engine [3]. Comparing the piston speeds of Lombardini LGA engine with HBO with the same sweeping volume at 4000 rpm (Figure 1.3), it can be seen that the piston of HBO engine moves more slowly around the top and bottom dead centers. However, the piston of LGA engine in the middle of its stroke moves at a higher speed for a short time in the maximum speed range of normal engines. As a result, the average speed of the piston of the HBO engine for the same crankshaft speed is lower than the average speed of the pistons of normal internal combustion engines, and the maximum crankshaft speeds of the HBO engines for the same average piston speeds may be higher. As a result of higher speed in the same engine dimensions, the power of the engine increases. Increased combustion time due to the low piston speed in the vicinity of the top dead center also extends the time required for the formation of the flame core, reducing the effect of local turbulence that will adversely affect the flame core. The velocity of the flame increases due to the lower volume increase during combustion. Due to the special structure of the connecting rod, the tangential force generated by the pressure generated in the cylinder from the start of the ignition occurs in the direction of rotation of the crankshaft, although the firing angle is before the top dead center relative to the piston [1].

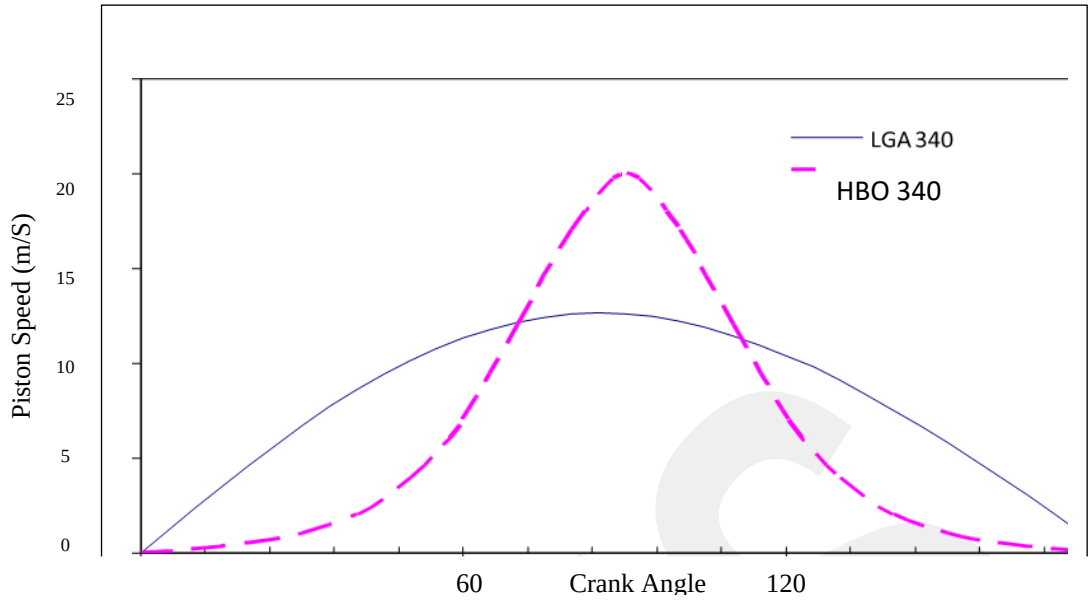

Figure1.3: Comparison of piston speeds of LGA and HBO engines [1].

1.2. Scope of The Thesis

The main objective of this thesis was to add electronic ignition and fuel injection systems to the engines, to use these systems as they were obtained from the market and to run and program them by providing completely empty ECU memory from the market. In this respect, the thesis has reached its target. Minisan has now decided to design all new prototypes with electronic ignition and fuel supply. They have found that the target was easily possible and that the cost was not high. Among its new prototypes is the 1600 cc two-cylinder and square-piston modular engine for cars. The main objectives of this study were:

1- The purpose of this thesis is the testing a relatively low cost engine that saves a high amount of fuel, resulting in higher power and torque in smaller cylinder volumes.

2- Comparing the values of the tested power, torque and specific fuel values of the HBO engine with the LGA engine.

3- Emission tests of HBO engine to minimize environmental pollution and comparison of these test results with the LGA engine results.

CHAPTER 2

LITERATURE REWIEW

2.1. Historical Background

In 1680, a Dutch physicist, Christian Huygens planned (yet never assembled) an inward burning engine that should have been filled with black powder.

In 1807, Francois Isaac de Rivaz of Switzerland invented an inside burning engine that utilized a blend of hydrogen and oxygen as fuel. Rivaz structured a vehicle for his engine - the main interior burning fueled car. Be that as it may, his was an extremely fruitless plan.

In 1824, an English engineer, Samuel Brown adjusted an old Newcomen steam engine to consume gas, and utilized it to quickly control a vehicle climbing up Shooter's Hill in London.

In 1862, Alphonse Beau de Rochas, a French structural architect, licensed, however didn't assemble, a four-stroke engine.

In 1866, German engineers, Eugen Langen and Nikolaus August Otto enhanced Lenoir's and de Rochas' structures and developed a progressively proficient gas engine.

In 1876, Nikolaus August Otto created an effective four-stroke engine, known as the "Otto cycle".

In 1885, Gottlieb Daimler developed what is frequently known as the model of the cutting-edge gas engine with a vertical chamber, and with gas infused through a carburetor (patented in 1887). Daimler had previously assembled a two-wheeled vehicle the "Reitwagen" (Riding Carriage) with this engine and after a year constructed the world's first four-wheeled engine vehicle.

In 1886, Karl Benz got the first patent (DRP No. 37435) for a gas-energized vehicle.

In 1890, Wilhelm Maybach fabricated the first four-chamber, four-stroke engine [4].

2.1.1. Developments in Internal Combustion Engines

The most important development in the last 25 years is the reduction of carbon dioxide emissions of internal combustion engines. Carbon dioxide emissions decreased from approximately 230 g/km in 1995 to 120 g/km at the present time. However, these levels are achieved with supercharged diesel engines. Low CO_2 emissions can be seen in the reduced gasoline engines in relatively higher models. The swept volumes of the engines must be reduced. This can be achieved by supercharging. Supercharging also increases efficiency in the diesel engine. However, it is aimed to reduce carbon dioxide emissions rather than increase in efficiency, since the air fuel ratio in the gasoline engine must remain within the combustible mixture range. In addition, over the last decade this technology has been evolved and overflowing have resulted in significant increases in the efficiency of small swept volume spark ignition engines. Due to significant engine speed changes in the urban usage, the turbochargers must be supported by a mechanical supercharge. These supercharging systems are becoming increasingly common. Along with turbocharging, reduction in internal friction provided by manufacturing techniques and material improvement, variable valve timing, fuel injection systems directly into the cylinder are also being applied [1].

The general trend continues to reduce engine swept volumes. This requires supercharging, electric motor support (hybrid) and weight reduction with the use of more carbon fiber material in chassis manufacturing. McLaren is working on mass production of carbon fiber usage in chassis manufacturing. With the use of carbon fiber, approximately twenty percent reduction in chassis weight is expected. As the swept volumes of gasoline engines decrease, it becomes difficult to maintain the desired torque in all engine speed ranges. Hybrid applications shall become applicable in this matter. With regenerative braking, extra torque is provided from the batteries that provide fast filling and the transitions in the speed ranges can be achieved. The McLaren P1 has such an application. Toyota has also focused on hybrid applications. Hybrid applications have different types as parallel and serial hybrid. Parallel hybrid applications have become widespread. The Toyota C-HR model, for example, applies a strategy of using only electric motors in urban traffic and using gasoline engines in non-urban areas. Generally, in parallel hybrid systems, the power of the vehicle is

provided jointly by gasoline engine and electric motor. For hybrid series applications, special spark-ignition engines are also designed which are called the range extender. These studies are still in prototype and development stage. This type of engine is designed to fit in the spare tire compartment in the rear trunk of the vehicle. In the hybrid series, the movement of the vehicle is provided entirely by the electric motor and the function of the spacer internal combustion engine is to charge the batteries by means of the generator. Both applications allow the vehicle to be charged at a station. The application of electricity is in the form of replacing 48-volt batteries with 12-volt batteries. With a 48-volt battery, it is possible to energize air-conditioning and other pumping systems and to provide independent support to idle and take-off systems without the support of the engine-powered alternator [1].

In addition, the turbocharging system will be added to the electric supercharge system, and twin-filling system will work more efficiently. Mazda has been awarded with a patent for the complete twin overfill system to be electrified. Accordingly, the second supercharge unit will automatically deactivate when the first reaches the desired speed. The General Motors (GM) Company plans to drive the supercharged unit with CVT (continuous variable transmission) unit. Infinity Company has produced a turbocharging and variable compression ratio engine for the QX50. This means that in economical driving mode, the turbo is deactivated and the compression ratio is increased, or the turbocharger and low compression ratio can be selected for high acceleration. This technology is expected to become widespread in the future. Finally, studies are being carried out on gasoline engines with compression ignition. Mazda announced in 2020 that the Mazda-3 series will use a SkyActive-X gasoline engine with compression ignition. At the point where the technology has come, it is possible in the future to design such vehicles with super lightweight, small swept volume, high speed, hybride assisted, carbon-based chassis with over-fill, variable suction and exhaust timing control, variable compression ratio, compression ignition and 48-volt battery assisted motor [1].

2.1.2. Suitable Fuel Types for Internal Combustion Engine

Advances in internal combustion engines have been developing in favor of spark-ignition engines with gasoline and gas. From a health point of view, the technological advances in diesel engines have also brought the end of urban use of these engines. Commercial medium and large diesel engines will continue to develop, but in areas where people live densely, diesel engines are now considered a health hazard. With the increase in fuel injection pressure and the reduction of the size of the particles in the exhaust gas, the microscopic particles coming out of the exhausts of diesel engines which seem to be working without smoke can reach the depths of our lungs and become trapped there and cause allergic reaction with carcinogenic unburned hydrocarbons. As a result of this, with the acceptance of the cause-effect relationship in increasing cancer cases by the world health organizations, the escape from diesel has started and will increase in cities. In our country, price adjustments are made to make the use of diesel vehicles more difficult. After a while the second hand prices of these vehicles will fall as a result of declining demand [1].

Internal combustion engines (ICE) have developed in parallel with technological development and especially in design, material and control has seen great advances today. The fuel economy and operational characteristics of ICEs are controlled electronically today. The control systems enable the control of the variables on the engine at different times during the operation of the ICE. Control systems further observes and controls whether the variables remain within the specified limits in accordance with the desired or planned values. Various data transmission systems are used to facilitate data transmission between control systems and to eliminate the need for excess cables [5]. In the study on the applicability of the electromagnetically controlled valve mechanism in a spark-ignition engine [6], an electromagnetic mechanism was prepared and prototyped for the opening and closing of the intake valve of a single-cylinder four-stroke spark-ignition engine at any time. The effect of various valve opening and closing times on the volumetric efficiency, torque, power, specific fuel consumption of the engine by changing the position of the Hail effect sensors on the engine was compared and compared with the classicly cam mechanism. It has been found that, due to the delay in the opening of the intake valve and the splashing of the valve and the disc, the electromagneticly controlled valve mechanism

causes a decrease in the volumetric efficiency, torque and power at high speeds and the mixing ratio deteriorates. An experimental motor with electro-hydraulic valve mechanism was created in the Ford research laboratory [7]. The new mechanism reduces the height and weight of the engine. Hydraulic power opens and closes both valves. Each cylinder has two intake and two exhaust valves. During the acceleration of the valve, the potential energy of the compressed fluid is converted to the kinetic energy of the valve, and during deceleration the kinetic energy of the valve returns to the fluid again. The recovery of kinetic energy in the electro-hydraulic system plays a key role in the low energy consumption of the mechanism [7].

2.1.3. Effect of Combustion on Engine Performance

Liquid and gas fueled engines use similar technology. Gasoline is the most widely used liquid fuel. The fuel is sprayed at multiple points in the intake manifold towards the intake valves via liquid fuel injection systems and the fuel vaporizes during the suction and compression strokes and is ignited by a spark of about 2000-2500 °C formed between the spark plug lugs about 20 degrees before top dead center towards the end of the compression. Since the fuel does not fully evaporate at this time and the combustion reaction is at the molecular level, a flame core delay occurs in the time it takes for the fuel droplets of hundreds of thousands of molecules to fully decompose into molecules. The flame core, which has grown sufficiently during this time, traverses the combustion chamber at a rate that starts and increases at a low rate and falls again, mainly due to the geometry of the combustion chamber and the turbulent movements of the gases. Since this process is fast and there is fuel stored in surfaces and recesses, some combustion continues after flame movement. There is no evaporation problem in gaseous systems, but there is a slight reduction in the amount of air absorbed as the fuel takes up more volume in the intake manifold. Experimental studies show that the decrease in volumetric efficiency is compensated by the increase in combustion efficiency. Generally, the octane numbers of gas fuels are higher than gasoline and compression rates around 13 are used in spark-ignition engines using natural gas. There are also systems where fuel is injected directly into the cylinders, but as the current situation of today's technology, these systems still need

improvement. Sufficient evaporation of the injected fuel during the firing phase is the most influential factor on the efficiency of combustion [1].

The most important factor affecting combustion is the flame speed. Therefore, the ignition takes place about 20 degrees before the TDC, so that the main stage of combustion spreads evenly around TDC. The part of the combustion in which the flame proceeds rapidly shows an approximate symmetrical distribution around the TDC. In this case, the pressure increase due to combustion before TDC has a negative effect against the rising piston. The angle at which the ignition is to be made is selected to provide an optimization in this respect. Generally, at the maximum torque position that the engine connected to the dynamometer can reach, this angle is determined for various operating modes and, in addition to the engine speed-accelerator pedal position, plus engine speed-intake manifold pressure, and in some applications additionally engine speed-oxygen sensor (lambda sensor) values are saved in ECU (Electronic Control Unit) memory as two-dimensional tables. Engines have been designed and prototypes have been built to control the movement of the piston independent of the crankshaft [8]. Thus, a constant volume of combustion is obtained. Due to the increased flame speed, it is possible to use better quality combustion and leaner mixture. However, the start of internal combustion engines depends on the adaptation of the reciprocating steam engine. The production, parts supply and maintenance costs of new types of mechanisms have limited these applications. The application that will bring the combustion closer to the fixed volume will be competitive if it occurs in the crankshaft-connecting rod-piston trio [1].

2.1.4. Effect of Volumetric Efficiency on Engine Performance

Oxygen is needed to burn the fuel, which is supplied by the air that is sucked in. As the content of oxygen increases, the combustion efficiency also increases, but twenty percent more air than the amount of air required for stoichiometric combustion determines the approximate limit for the lean mixture. Even if more air increases the combustion efficiency to some extent, the flame may not proceed properly in the mixture with the diluted fuel and may even be extinguished. This limit can be increased with some combustion chamber geometries and direct injection systems. One way to

increase the amount of air is supercharging. However, since the way to reduce specific fuel consumption is to achieve the same performance with less fuel, the increase in combustion efficiency must offset the reduction in energy entering the system due to the reduction in fuel quantity. The opening and closing angles of the intake and exhaust valves play an important role in this stage. In general, the suction valve is opened before the TDC to prolong the fully open duration of the camshaft-driven valves. In some modern engines, the opening angle is variable. The exhaust valve is opened before the bottom dead center (BDC) and the useful work of the expanding gases is reduced, in order to more easily exhaust gases. The closure of the intake and exhaust valves after BDC and TDC is in order to benefit from the inertia of the moving gases. If variable on-off angle control is not applied, these angles are adjusted for high speeds and therefore at low speeds some exhaust gas enters the early opening suction valve and some of the suction air fuel mixture escapes from the still open exhaust valve and some of the suction air fuel mixture is rising it escapes from the suction valve which is still open by the piston. Engines designed to control the movement of the intake and exhaust valves independently of the movement of the piston have been designed. An application that will allow the suction and exhaust valves to open and close around the BDC and TDC will gain competitiveness if realized in the crankshaft-connecting rod-piston trio [1].

2.2. Development of Engine

There are three main objectives required to be achieved in the development of an internal combustion engine. These are respectively high specific power, low specific fuel consumption and low specific harmful emissions. Specific power is the power generated by the engine in relation to the swept volume, specific fuel consumption is the fuel consumed by the engine compared to the power produced, and specific harmful emissions are harmful gases emitted to the atmosphere by the engine according to the swept volume. Since internal combustion engines derive their energy from the chemical energy of the fuels they use, their specific power depends on the amount of fuel they use per unit time.

2.2.1. High Specific Power

In order to increase the specific power, it is necessary to obtain the same power from a smaller engine. For this, it is necessary to increase the amount of air entering the engine and thus the fuel. Mechanical supercharging and turbo supercharging systems are applied to increase specific power. The compressed air is cooled by passing it through a separate heat exchanger before entering the intake manifold. Thus, by increasing the density, more air mass is introduced into the intake manifold. While mechanical supercharging systems derive their energy from the crankshaft of the engine, the energy of exhaust gas is utilized in turbo charging systems [9].

In these engines, the fuel is injected into the intake port towards the intake valve. This provides easier electronic control and allows the air/fuel mixture to cover the intake manifold more. In this way, the dynamic reaction of the system is improved and fuel supply delays are reduced. The turbocharger system has been used for a long time in diesel engines and is very advanced. However, in spark ignition engines, the emission control was successfully carried out by three-way catalytic filters, while the turbocharger system was regarded as a luxury. When reducing CO2 emissions became important, it was also important to reduce the size of spark-ignition engines. Computer-based models for turbo charging systems were developed using finite element analysis [10]. In the turbocharger application, the exhaust gas to the turbine must be controlled by the escape valve. As an ideal control strategy, control models have been developed based on the approximation of the compressor outlet pressure and the outlet pressure of the throttle valve at the intake manifold inlet as close as possible [11]. Due to the inertia of the turbocharger system, the desired torque is delayed in comparison to naturally aspirated engines. There are three methods to correct this important disadvantage. The first method is to place an additional suction valve on the cylinder head and pump air from there during the transition period [12]. This method is both complicated and costs too much. The second method is to place an additional intake valve on the intake manifold and pump air from there during the transition period [13]. Although this method is relatively less complicated and costly, an extra compressor is needed. Both methods require pneumatic control. The third method is to use an auxiliary system that will provide additional power to the engine

during the transition period. As an auxiliary system, the electric motor can be used in hybrid vehicles or a second mechanical supercharger can be activated.

2.2.2. Low Specific Fuel Consumption

In general, the mass air / fuel ratio is between 12 to 18 in spark ignition engines. This ratio may be higher for some engines. Direct fuel injection technology, defined as GDI (Gasoline Direct Injection) working with leaner mixtures, has been introduced by various companies [14]. A comparative and detailed review of these systems was conducted [15]. Compared to fuel injection systems behind the intake valve, there is no fuel wetting behind the intake valve by spraying the fuel directly into the cylinder and the flow rate of the fuel can be controlled more precisely. With the GDI system, leaner air / fuel mixtures can be used, operation without the air throttle is possible, air / fuel differences between the cylinders are reduced and specific fuel consumption is reduced. Due to the high fuel injection pressure of the GDI system, the diameter of the fuel droplets in the cylinder is reduced from an average of 120 microns to 16 microns. In the study conducted on Nissan engine [16], it was determined that unburned hydrocarbon emissions decreased by 30% during cold working. However, GDI systems also have some disadvantages. It is difficult to control the diluted air/fuel ratio over the entire operating range of the engine. Complex control and fuel injection technologies are needed to accommodate load changes. Relative deposit build-up increases in injectors and spark plugs. Unburned hydrocarbon emissions are relatively increased at partial loads. Oil-carbon deposit is formed at high loads. Particle emissions are increasing. Three-way catalysts cannot be used in their full form. Due to the high pressure of the fuel and low oiling viscosity, the wear of the components in the fuel supply system increases. The inner walls of the cylinders are becoming more worn out. More power and higher voltage is needed for injectors and its drivers. The fuel supply pressure is fluctuating. However, GDI systems have shown continuous improvement. In the beginning, fuel systems have been adapted from diesel engines. The Texaco TCCS engine [17] uses a high penetration and relatively low atomization diesel injector. The Ford PROCO engine [18] used a relatively low-pressure outward-sloping single-bore diesel injector. The common feature of these types of injectors was the high unburned hydrocarbon emissions in cold operation due to high penetration.

As the research continued, it has been determined that the injected fuel must have a stable and aggregate geometry in order to efficiently burn the diluted air / fuel mixtures. Mitsubishi developed fuel supply strategies [19]. Thus, common fuel feed pipe and electromechanical activation systems were developed [20]. Another way to achieve a lean mixture in internal combustion engines is the orientation of intake manifold inlets and combustion chamber designs to provide graded filled combustion [21]. In the study that was carried out at METU, the cylinder head of 131 engines of 4 cylinders and fuel injection gasoline produced by TOFAŞ was reworked as horizontal after filling with aluminum alloy welding. The suction ports are also redesigned to give the suction air a loop motion and mold cores are produced to cast new cylinder heads. After the heads processed in TOFAŞ, the combustion chambers were reworked. The engine was able to run with 76 octane gasoline without knocking and the air/fuel ratio increased to 22 [1].

In a study carried out in the research engine, it was found that the differences between the cycles occurred in the combustion gas mass up to five percent especially in the vicinity of the spark plug in the stepper engines [22]. Although stepwise filled engines and lean mixtures are obtained, they are not yet widely used because of the same driving comfort in the entire operating range. Working with a lean mixture also has the effect of reducing specific harmful emissions. Carbon monoxide and unburned hydrocarbon emissions are reduced due to improved combustion quality. NO_x emissions are also reduced due to the cooling effect of increased nitrogen in the air [9].

2.2.3. Low Specific Harmful Emission

The most important development in the last 25 years is the reduction of carbon dioxide emissions of internal combustion engines. Carbon dioxide emissions decreased from approximately 230 g/km in 1995 to 120 g/km at the present time. However, these levels are achieved with supercharged diesel engines. Low CO2 emissions can be seen in the reduced gasoline engines in relatively higher models. Exhaust emissions from internal combustion engines are one of the major causes of environmental pollution. The reduction in the use of fossil fuels and increasing environmental pollution have led to the search for alternative and renewable fuels that are environmentally friendly and

more efficient engine technologies. It is desirable that the investigated alternative fuels are capable of reducing exhaust emissions without reducing the performance of the internal combustion engine. It is also important that this fuel is available, cost-effective, usable, available and used without requiring much modification to the engine. Their emissions were measured by the AVL system [1]. In this thesis CO_2, CO, O_2 and hydro carbon emissions of HBO engine are measured and plotted.

Figure 2.1: AVL system.

2.3. Effect of Compression Ratio on Efficiency in Internal Combustion Engines

The system continuously and independently controls most of the parameters of the valve movement. It allows the optimization of valve events for all operating situations. The effect of compression ratio on the efficiency of engines is quite high. Compression ratio can be increased with high octane number [23]. Therefore, the advantage of LPG is seen as a high compression ratio to prevent knocking and low exhaust emissions. The effect of specific fuel consumption and engine power was investigated by increasing the compression ratio of a spark-ignition engine operating with LPG [24]. With an increase in the compression ratio from 9.5 to 13; average fuel consumption decreased by approximately 12% and engine power increased by approximately 7%.

A good variable compression ratio mechanism needs to provide certain properties; the system should be simple, small in size and light, should not pose a serious design problem, the compression ratio should be able to be varied in all ranges and should be used in piston engines, the compression ratio should be precisely adjusted, the other engine parameters should not cause undesirable changes, the balance of the engine should not deteriorate compared to the classic engine and the engine life should not be shortened. In a 4-cylinder 1.6-liter cylinder volume Otto-Atkinson (OA) cycle, the compression ratio is changed by a piston with variable compression height [25]. 15% reduction in specific fuel consumption compared to standard engine. Thermodynamic calculation and experimental study to determine the factors limiting the improvement in the thermal efficiency of spark ignition engines at high compression rates were found to be the main factors cooling losses and unburned fuel [26]. It has been explained that these two factors increase in small cylinder volumes, large surface / volume ratio combustion chambers, low engine speed and load. A simulation model has been developed to examine parameters such as equivalence ratio, ignition timing, compression ratio, compression and expansion index that affect 4-stroke spark ignition engine performance [27].

In a theoretical study, different power and efficiency characteristics were calculated with a motor power cycle model for different compression ratios [28]. Engine performance can be optimized in all driving conditions; It is suggested that high compression ratio should be used at low power levels in order to benefit from fuel efficiency and low compression ratio should be used to avoid pinking at high power levels. In the study performed with Ricardo E6 engine with single cylinder variable compression ratio, the output power was increased from 8 to 11, resulting in an improvement in output power of approximately 22% [29]. It has been observed that with the increase of compression ratio, the increase of end-compression temperature and pressure and the decrease of residual gases, the combustion time is shortened, the combustion rate increases and the ignition delay is decreased [30]. In this study, the effects of the change of compression ratio of a four-stroke, single-cylinder engine with spark plug ignition on engine performance and exhaust emissions were investigated experimentally. Average effective pressure increase, increase in engine torque and

power and decrease in specific fuel consumption were determined by increasing the compression ratio [23].

Investigating the possibilities of improving the performance of a single cylinder engine with low power and efficiency and reducing emission values [31], the compression ratio of the engine is increased from 5 to 9, with 44% torque increase at maximum torque speed (2000 rpm) and 32% power increase at maximum power speed (3500 rpm) when working with LPG at maximum compression rate. In order to optimize combustion with a variable compression ratio engine, a 4-stroke, 4-cylinder, gasoline-injected engine was changed the compression ratio in the range of 9.5 to 15 by the addition of an auxiliary combustion chamber to the cylinder head depending on the speed and load. The compression ratio was changed by a movable piston placed in the auxiliary combustion chamber. In the experiments carried out with the vehicle which is converted to a variable compression ratio engine, the fuel consumption of partial loads has been reduced by up to 12%. In addition, a decrease in CO and NO_x emissions and an increase in HC emissions were determined [32]. In a gasoline engine with a stepped combustion chamber designed and manufactured with prototypes, compression ratio was increased and knocking was prevented. It has been shown that this type of engine can operate without knocking with 76 Octane gasoline [33].

2.4. Common Factor Combustion Efficiency

Combined efficiency is the common factor in achieving high specific power, low specific fuel consumption and low specific harmful emission targets. In spark ignition engines, the properties of the in-cylinder gas during ignition directly affect the combustion efficiency. The entire duration of combustion is influenced by the formation of the flame core [34]. Depending on the combustion speed, the maximum speed and therefore the maximum power of the motor is limited. As the combustion rate increases, the pressure differences between the cycles decrease, the knock decreases, and changes in torque requirements can be achieved faster. However, due to the geometry of the piston-connecting rod-crankshaft, the residence time of the piston around the top dead center decreases as the speed of the crankshaft increases. Ignition is performed before the top dead center to prevent combustion from sagging

too much on the expansion stroke. As the speed of the crankshaft increases, the ignition time is gradually increased from the top dead center. Thus, in the initial stage of combustion, the increased pressure of the combustion gases against the piston, which moves towards the top dead center on the compression stroke, creates extra resistance. The ignition time must always be set to the optimum point according to the operating modes of the engine. In most engines, ignition angles are determined by ECU according to the operating mode of the engine using tables obtained from performance and mapping experiments [35].It is also possible to determine the continuous firing angle with feedback using a knock probe to operate the engine continuously at maximum torque position and at the knock limit [36].

The most important development achieved with this project has been the application of the ignition advance beyond the mechanically achievable ignition advance degrees in normal engines. It was thus possible to make better use of the different piston movement and speed resulting from the geometry of the crankshaft of the HBO engine. However, the valve timing and combustion chamber geometry must also be redesigned [1].

CHAPTER 3

MATERIAL AND METHODS

3.1. Experimental Set-Up

3.1.1. Eddy Current Dynamometer

Atılım University Automotive Engineering Department Engine Laboratory has three separate engine test rooms with 40 kW, 160 kW and 350 kW loading capacity Eddy-current dynamometer. The dynamometers are controlled by the BME (Dynamometer Control Unit) unit (Figure 3.1). This unit includes motherboard and serial communication circuits with Intel processors and control circuits of the power unit [1].

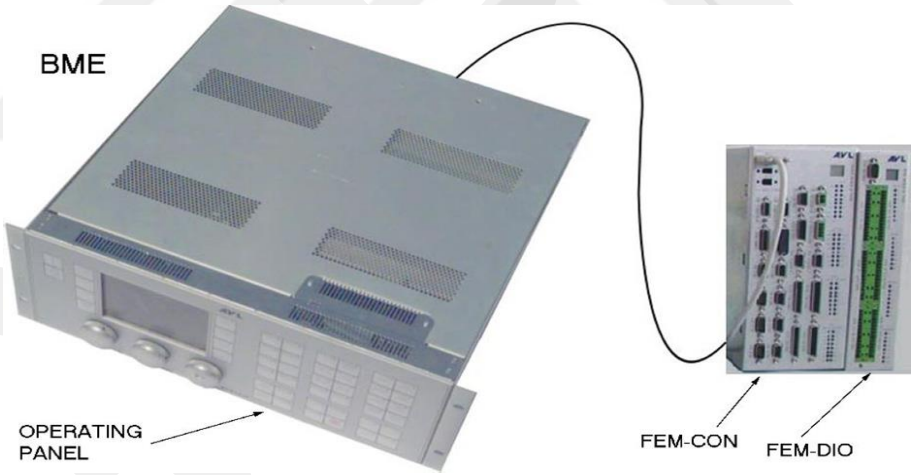

Figure 3.1: AVL control units BME, FEM-CON and FEM-DIO [1].

FEM-DIO, where dynamometer and power unit and digital circuits used for communication and data transfer, and FEM-CON units with digital-analog converter circuits communicate with the BME unit via serial port. To control the BME unit from outside the system, the Emcon Remote Interface Collection (ERIC) library, which is

written in C++, communicates over the serial port. All units, including this test computer, are collected in a console outside the test chamber (Figure 3.2) [1].

Figure 3.2: Single cylinder test control console.

3.1.2. Control of Dynamometer

A program (Test) was written with Borland C ++ Builder6 to control the BME unit using the ERIC library. This program is object-oriented and has a visual interface. The program uses Advantech 1716 data card for digital signal input-output and analog signal output for collecting, processing and controlling data and searches for this card at power-up. Once the card is found, the meeting protocol is applied. When this stage is successful, the ".xml" file is searched and applied. The test type is then selected and the test interface is opened.

At this stage, the type of the experiment is selected as performance or mapping from the experiment menu and a panel is opened at the beginning of the experiment report where information about the engine and the experiment is specified. After filling in this information, activation of the electrical circuits controlling the dynamometer and the internal combustion engine starts (Figure 3.3).

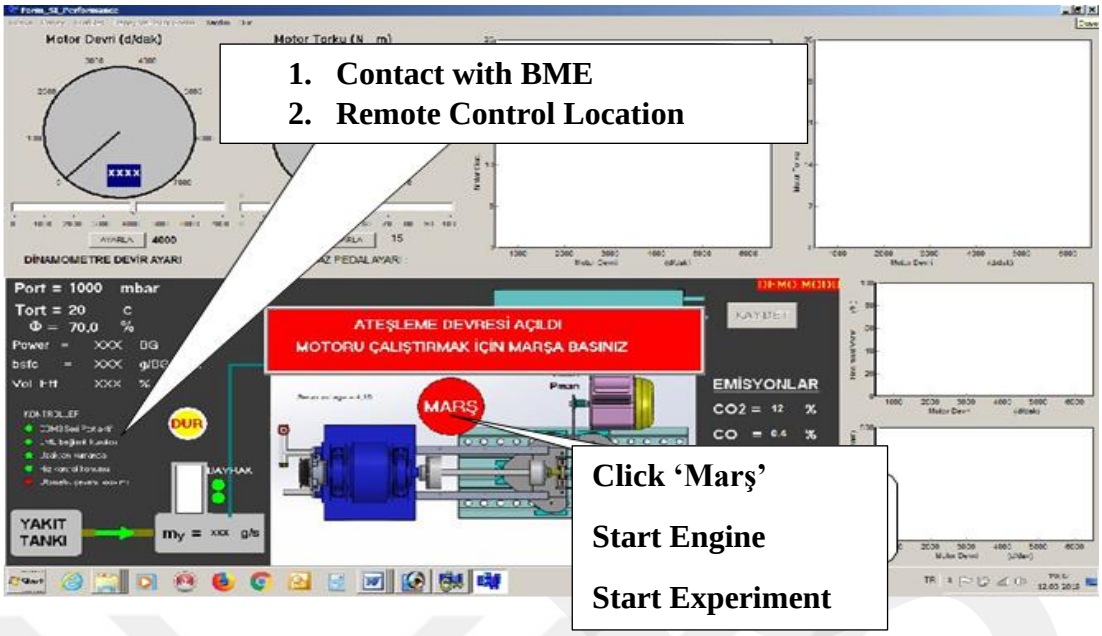

Figure 3.3: Initial phase of the test program.

This is executed via serial port and Advantech data card. However, it is inconvenient that this card communicates directly with electromagnetic recoil circuits such as relays. An interface circuit was designed for this communication and the printing circuit was manufactured.

An amplifier circuit was designed to amplify the signals from thermoelements and other low signal level sensors and the printing circuit was manufactured. The interface, fuel metering and power supply circuits are combined in a single box. Separate boxes for the amplifiers were manufactured [1].

3.1.3. Torque and Fuel Measurement System

The single cylinder HBO engine was connected to a 40-kW dynamometer (Figure 3.4) by means of a special apparatus. The problem of matching the axes of the crankshaft of the engine and the shaft of the dynamometer is solved with the chain link (Figure 3.5). The force sensor used by the dynamometer to measure torque failed at the beginning of the experiments.

Figure 3.4: 40-kW dynamometer [1].

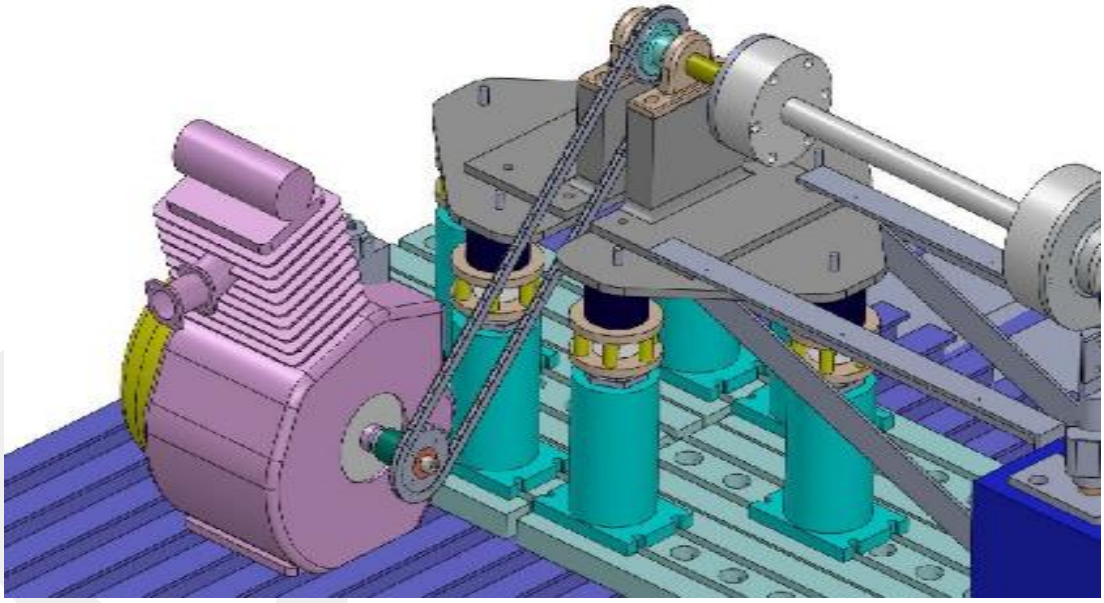

Figure 3.5: 40-kW dynamometer, special apparatus and chain link.

The OMEGA PX309 pressure sensor in the laboratory was fitted to the brake outlet of the caliper (Figure 3.6). By loosening the bleed valve of the caliper, hydraulic fluid was delivered from here with the syringe and the system was vented into the filling chamber.

Figure 3.6: Pressure sensor [1].

In this case, the system was reset and it was statically calibrated with the weights placed on the torque arm of known length. Since the PX309 sensor output is 0-5 vdc, a voltage divider circuit is added to the output of the circuit and a signal is sent to the FEM CON circuit to which the BME unit controlling the AVL dynamometer is connected. The resistance of the divider circuit was adjusted to be read on the 50.5 N-m BME display corresponding to a maximum weight of 13.2 kg. The calibration curve was then generated by removing the weights sequentially and then increasing it. The calibration method was the same as applied by AVL for the original force sensor. The mean of the hysteresis of increasing and decreasing weights was used. The engine speed was measured by the position sensor connected to the dynamometer and the gear on the dynamometer shaft. In this way, the torque and speed of the motor were directly measured by the BME unit and transferred to the computer program controlling the experiment with the ERIC software and the power of the motor was calculated [1].

A specific measurement system (Figure 3.7) was designed for fuel measurement. In this system, solenoid valves were connected to the inlet and outlet of a cylinder with a diameter of 10 cm and a height of 20 cm. The solenoid valve at the outlet is required for static calibration.

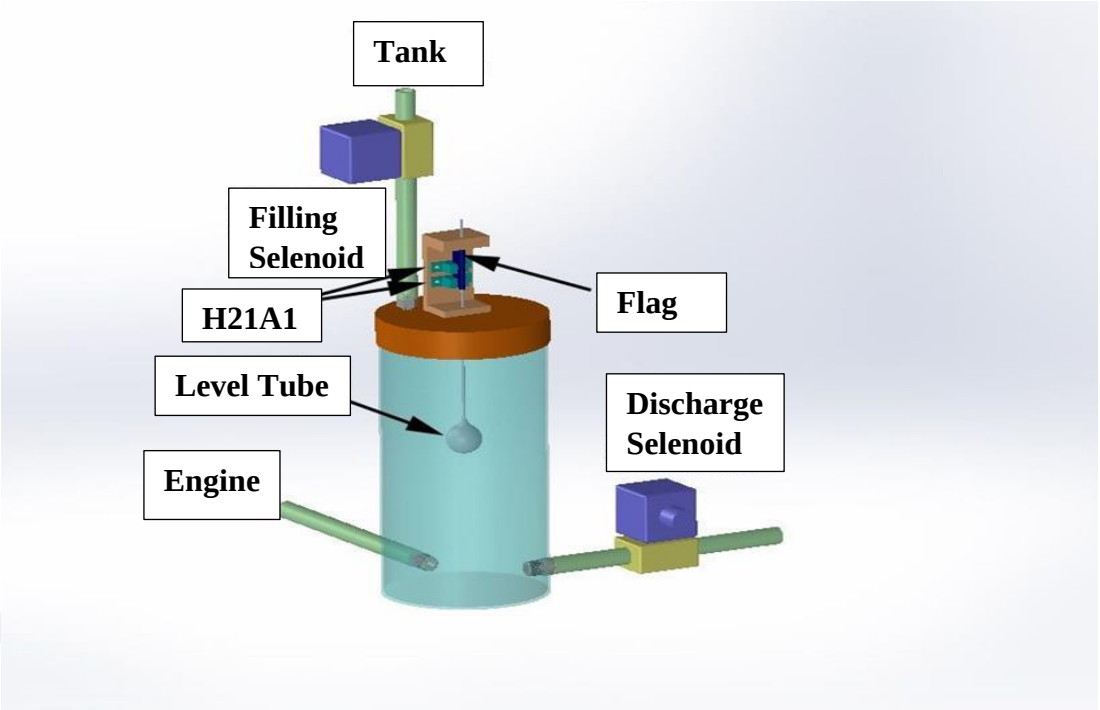

Figure 3.7: Fuel metering system.

A circuit was designed for the automatic opening and closing of the solenoid valves by triggering the cross-section of the flag in and out between the H21A1 sensors, while measuring the time taken to consume a certain volume of fuel and the PCB circuit was produced.

Using this circuit, a program which can be repeated up to ten times and calculates the average and gives one full fuel consumption was prepared (Figure 3.8). During the experiments, the fuel consumption was repeatedly measured by automatically trigering the top and bottom H21A1 as the cylindrical reservoir was disharged and filled. In this measurement system, the temperature of the fuel in the cylindrical reservoir can be controlled by a thermistor and the heating or cooling water flow in the copper spiral pipes passing through the reservoir can be controlled. The fuel metering system is designed to operate in two different modes. The computer-controlled version was used in the experiments. In addition, a self-running and self-measuring version using a 74LS74 flip-flop was also created.

Figure 3.8: Fuel calibration program.

3.1.4. Engine Accessories

A servo motor was adapted on the throttle of the motor (Figure 3.9). Arduino MEGA 2560 and servo motor control software were added to the computer program via serial port. The supply voltages of the servo motor in the throttle fully closed and fully open positions were set above the mid-point of the 0-5 vdc range. Accordingly, it is necessary to give 4.40 volts to the servo motor when the throttle is fully closed, and to give 2.80 volts even though the throttle is fully open. Accordingly, the output voltage ranging from 2.80 to 4.40 volts is supplied to the ECU to control electronic ignition coils and electronic fuel injection injectors with engine speed [1].

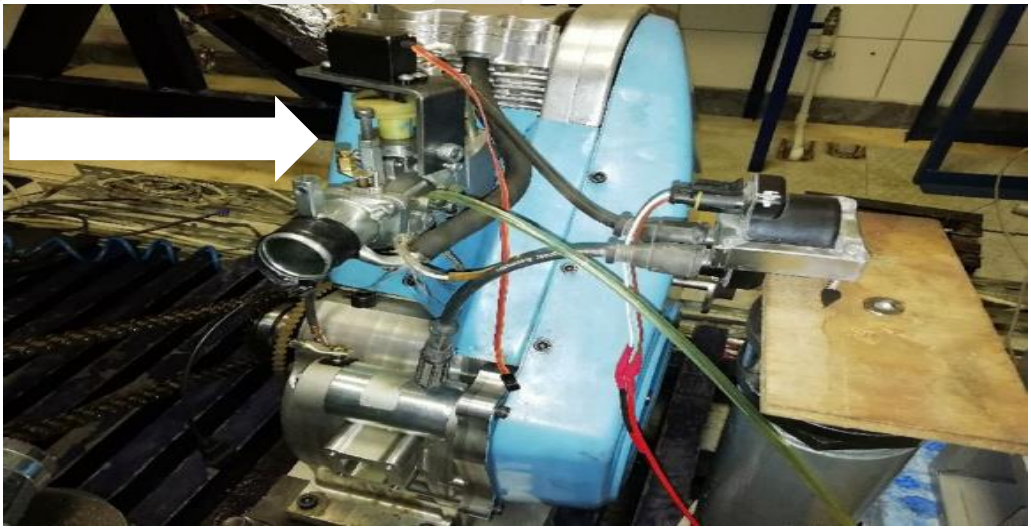

Figure 3.9: Servo motor on the throttle [1].

Ignition angles and fuel injection times were made according to the mapping tables previously created. Fifty-eight gear and magnetic sensors were added to the output shaft to transfer the crank angle and speed of the engine to the ECU. BOSCH HFM 5 (Figures 3.10) type sensors were added to the intake duct for air flow.

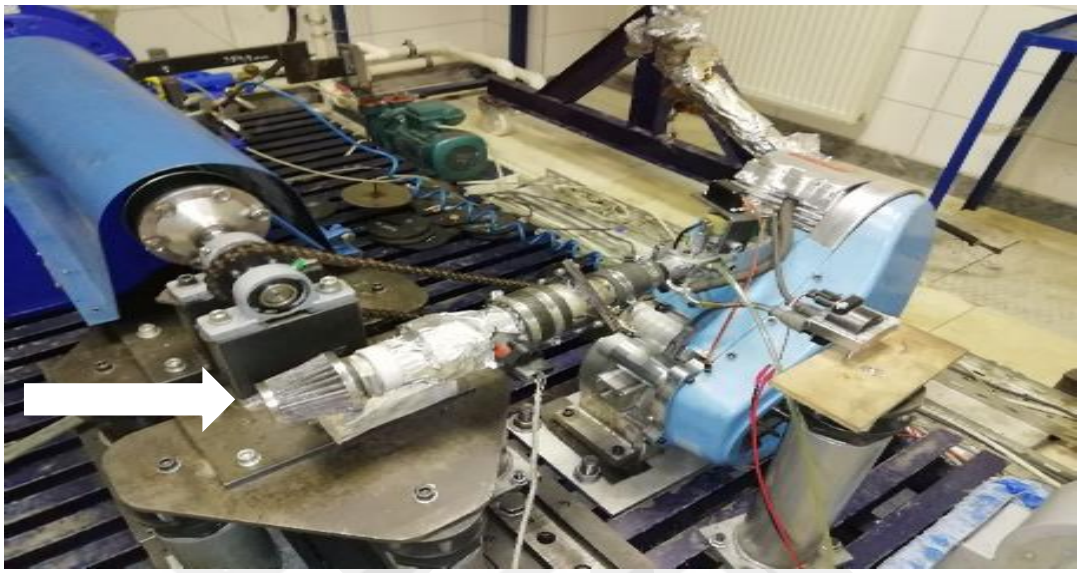

Figure 3.10: Flowmeter.

3.2. Experimental Method

3.2.1. Calibration of Designed Force Sensor

On the arm extending from the dynamometer for calibration, holes were drilled not exceeding the body of the dynamometer and a cylinder was placed on these holes to apply pressure to the central piston of the caliper. The portion of the cylinder coming to the arm was machined (Figure 3.11). For calibration, approximately equal weights of up to 13.2 kg in weight were placed on the weight suspension plate at a distance of 389.9 mm and the corresponding torque values were recorded. In this way, the torque readings corresponding to the torque values corresponding to approximately equal weights up to a torque of about 50.5 N-m were recorded.

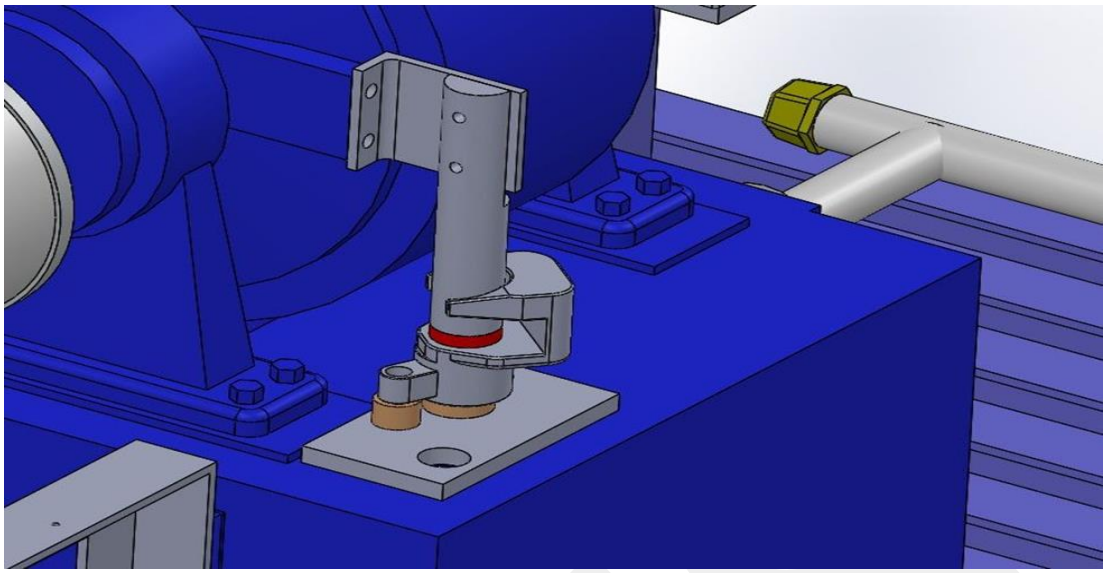

Figure 3.11: Connection between pressure sensor and dynamometer.

3.2.2. Calibration of The Fuel Metering System

Before starting the experiment, the hose tare at the outlet of the discharge solenoid of the fuel metering system was introduced into a weighed one-and-a-half-liter pet water bottle. Liquid Fuel Measurement Calibration was selected from the Test Type menu in the test program. In this position, two of the digital outputs of the program Advantech data card triggered channels in the ULN2003 circuits via the 74LS245 circuit in the interface circuit. The triggered ULN2003 channels triggered the respective solenoids by releasing the trigger legs of the respective relays into the ground. These operations were performed with the following code that started when clicking the start button.

3.3. Experimental Study

3.3.1. Manual Test Study

When you select HBO single- or double-cylinder test from the Experiment Type menu on the opening page, it is necessary to start by selecting the experiment type on the new page. Then, after determining the file to save the data, the panel where the general

experiment information is entered into is opened and the Experiment menu is activated.

After making the necessary settings in the Experiment menu, the Start Experiment tab is selected from the menu. At this stage, the Test program sends commands to the solenoid related to the data card and interface circuit.

In each of the test assemblies in three separate test chambers, electric motors connected to the shaft of the dynamometer by belt and pulley were attached. The connections of the pulleys to the dynamometer shaft are also provided with magnetic couplings. The test program first sends a digital signal to the relay running the electric motor and waits for five seconds and then sends a signal to the relay connected to the magnetic coupling. In this way, the first movement is given to the motor connected to the dynamometer without using the starter motor. The test program monitors the speed data output from the BME unit after sending the signal to the magnetic coupling, and when the specified speed is exceeded, it first cuts the circuits of the magnetic coupling and then the electric motor.

The engine starts in idle mode. After waiting for the 5 seconds, the first engine and dynamometer settings are made to start the experiment. At this stage the test program performs the routing.

The experiments will continue automatically or manually depending on the selection in the Experiment Menu. The test results are prepared in a table and saved in the format to be exported to the excel file.

3.3.2. Data Processing

Performance experiments were performed at various gas throttle positions. The throttle position was kept fixed and the torque was measured at six different positions at equal intervals between the maximum and minimum speeds. Engine speed, torque, fuel consumption, air consumption, air inlet temperature, ambient air temperature, pressure, humidity and water inlet and outlet temperatures were measured at each measurement position. In addition, the position of the throttle with the signal from the servo motor control circuit was also recorded. This process can be done manually or

automatically. Since the maximum engine speed was determined, 1000 rpm was selected as the minimum engine speed and the measurements were repeated at equal intervals. At the beginning of the experiment, the independent measurement of fuel measurements was accepted as a prerequisite for recording the measurements. Preliminary tests have shown that the three fuel measurements provide sufficient stability. The difference between the second and third fuel consumption readings remained below two percent.

The values in the exemplary experiment were obtained at the end of the third fuel measurement. In the experiments, the ignition advance and fuel flow could be controlled independently. However, in experiments with the carburetor, the fuel flow could be controlled by a needle moving in the orifice and approximate parametric experiments could be carried out by changing fuel consumption because the position of the needle was affected by the vibrations of the engine and the repeatability of the central position in the orifice was low. Nevertheless, large increases in specific fuel consumption have helped identify faulty areas.

The mapping experiments were obtained by repeating performance tests at different throttling positions. The angle between the full throttle angle and the idle angle was reduced to ten different sections, and performance tests were repeated at the throttle positions up to ten percent of this range. These data were matched to quadratic curves and the speed range was divided by equal intervals and torque values at the same speed were interpolated between the curves for the selected throttle positions. In this way, tables containing torque values relative to throttle position and speed were created [1].

3.3.3. Preparation of ECU Tables

The GEMS EM36 ECU is programmed for the single-cylinder HBO engine. For this purpose, static tests were performed to measure the fuel injection flow rate of the injector and the fuel times were calculated.

After the preliminary tables were created, the engine was started with these values and renewed with the tables obtained as a result of the experiments. Service was obtained for the two-cylinder engine and the engine was started with KINGZ brand ECU. Carburetor tests of this engine were not performed and they were operated directly with ECU by installing electronic ignition and fuel injection system [1].

3.4. Calculations

3.4.1. Calculating Torque

The torque at the crankshaft is produced by the force applied on the connecting rod journal through the connecting rod. The torque "T" will be produced at the crankshaft on each connecting rod journal, every time the piston is in the power stroke. The lever arm in this case is the crank radius (offset). The magnitude of the force "F" depends on the combustion pressure in the cylinder. The higher the pressure in the cylinder, the higher the force on the crankshaft, the higher the output torque. The length of the lever arm has impact on the overall engine balance. Increasing it too much can lead to engine imbalance, which results in higher forces in the crankshaft journals [6].

The area of the piston (assuming the the piston head is flat and its diameter is equal with the bore of the cylinder) is:

$$\boldsymbol{A_p = \frac{\pi}{4} B^2} \qquad \textbf{(3.1)}$$

The force applied to the piston is calculated as follows:

$$\boldsymbol{F = p \times A_p} \qquad \textbf{(3.2)}$$

Where p is the pressure inside the cylinder. Assuming that all the force in the piston goes into the connecting rod, the torque is calculated as:

$$\boldsymbol{T = F \times a} \qquad \textbf{(3.3)}$$

Torque T [N.m] can also be expressed as a function of the mean effective pressure of the engine [6]:

$$\boldsymbol{T = mpe \times V_d \times 2nr} \qquad \textbf{(3.4)}$$

where:

mep [P_a] – mean effective pressure

V_d [m^3] – engine displacement (volume)

nr [-] – number of crankshaft revolution for a complete engine cycle (for a 4-stroke engine nr = 4)

3.4.2. Calculating Power

In physics, power is the work done in time or, with other words, is the rate of doing work. In rotational systems, power P [W] is the product of the torque T [N_m] and angular velocity ω [rad/s] [6].

$$\boldsymbol{P = T \times \omega} \quad \textbf{(3.5)}$$

The standard unit of measurement for power is W (Watt) and for rotational speed is rad/s (radian per second). Most of the vehicle manufacturers are providing the power of the engine in bhp (brake horse power) and the rotational speed in rpm (rotations per minute). Therefore, we are going to use conversion formulas for both rotational speed and power [6].

To convert from rpm to rad/s, we use:

$$\boldsymbol{\omega[rad/s] = N[rpm] \times \frac{2\pi}{60}} \quad \textbf{(3.6)}$$

To convert from rad/s to rpm, we use:

$$\boldsymbol{N\ [rpm] = \frac{\omega[rad/s] \times 60}{2\pi}} \quad \textbf{(3.7)}$$

The engine power can also be measured in k_W instead of W for a more compact value. To convert from k_W to bhp and reverse, we use:

$$\boldsymbol{P[bhp] \times P[kW] = 1.36 \times P[kW] = P[bhp] \times 1.36} \quad \textbf{(3.8)}$$

In some cases you might find HP (Horse Power) instead of bhp as unit of measurement for power.

Having rotational speed measured in rpm and torque in N_m, the formula to calculate power is:

$$\boldsymbol{P[kW] \times p[HP] = \pi \times n[rpm] \times T[Nm] \times 30 \times 1000 = 1.36 \times \pi \times N[rpm] \times T[Nm] \times 30 \times 1000} \quad \textbf{(3.9)}$$

3.4.3. Calculating Specific Fuel

The approach is to calculate how much fuel would be necessary for stoichiometric combustion in each cylinder, assuming that each cylinder is filled with air at atmospheric pressure (100% volumetric efficiency). The fuel quantity for idle conditions is then calculated for an expected typical MAP value at idle [6].

$$\boldsymbol{Mass\ of\ air = m_a = \frac{PV}{RT}} \quad \textbf{(3.10)}$$

$$\boldsymbol{Mass\ of\ fuel = m_f = \frac{m_a}{AFR}} \quad \textbf{(3.11)}$$

For gasoline of Specific Gravity of 0.75

$$\boldsymbol{Volume\ of\ fuel = V_f = \frac{m_f}{0.735\frac{kg}{l}}} \quad \textbf{(3.12)}$$

3.4.4. Calculating Specific Air

For a thermal engine, the combustion process depends on the air-fuel ratio inside the cylinder. The more air we can get inside the combustion chamber, the more fuel we can burn, the higher the output engine torque and power [6].

Since air has mass, it has inertia. Also, the intake manifold, the valves and the throttle are acting as restrictions for the air flow into the cylinders. By volumetric efficiency we measure the capacity of the engine to fill the available geometric volume of the

engine with air. It can be seen as a ratio between the volume of air drawn the cylinder (real) and the geometric volume of the cylinder (theoretical) [6].

Most of the internal combustion engines used nowadays on road vehicles, have a fixed volumetric capacity (displacement), defined by the geometry of the cylinder and the crank mechanism. Strictly speaking, the total volume of an engine V_t [m^3] is calculated as a function of the total number of cylinders nc and the volume of one cylinder V_{cyl} [m^3] [6].

$$\boldsymbol{V_t = nc \times V_{cyl}} \quad \textbf{(3.13)}$$

The total volume of the cylinder is the sum between the displaced (swept) volume V_d [m^3] and the clearance volume V_c [m^3].

$$\boldsymbol{V_{cyl} = V_d + V_c} \quad \textbf{(3.14)}$$

The clearance volume is very small in comparison with the displacement volume (e.g. ratio 1:12) so it can be neglected when calculating the volumetric efficiency of the engine [6].

IV – intake valve

EV – exhaust valve

TDC – top dead center

BDC – bottom dead center

B – cylinder bore

S – piston stroke

r – connecting rod length

a – crank radius (offset)

x – distance between the crank axis and the piston pin axis

θ – crank angle

V_d – displaced (swept) volume

V_c – clearance volume

The volumetric efficiency η_v [-] is defined as the ratio between the actual (measured) volume of intake air $_{Va}$ [m^3] drawn into the cylinder/engine and the theoretical volume of the engine/cylinder $_{Vd}$ [m^3], during the intake engine cycle [6].

$$\boldsymbol{\eta v = V_a \times V_d} \quad \textbf{(3.15)}$$

The volumetric efficiency can be regarded also as the efficiency of the internal combustion engine to fill the cylinders with intake air. The higher the volumetric efficiency the higher the volume of intake air in the engine [6].

In case of indirect fuel injection engines (mainly gasoline) the intake air is mixed with fuel. Since the amount of fuel is relatively small (ratio 1:14.7), compared with the amount of air, we can neglect the fuel mass for volumetric efficiency calculation [6].

The actual intake air volume can be calculated function of air mass ma [kg] and air density ρa [kg/m^3]:

$$\boldsymbol{V_a = m_a \times \rho_a} \quad \textbf{(3.16)}$$

Replacing (5.17) in (5.16) gives the volumetric efficiency equal to:

$$\boldsymbol{\eta_v = (m_a \times \rho_a) \times V_d} \quad \textbf{(3.17)}$$

Usually, on the engine dynamometer, intake air mass flow rate is measured [kg/s] instead of air mass [kg]. Therefore, we need to use air mass flow rate for volumetric efficiency calculation [6].

$$\boldsymbol{m \times a = m_a \times N_e \times nr} \quad \textbf{(3.18)}$$

where:

N_e [rot/s] – engine speed

n_r [-] – number of crankshaft rotations for a complete engine cycle (for 4-stroke engine nr = 4)

From equation (5.19), we can write the intake air mass as:

$$\boldsymbol{m_a = m \times a \times nr \times N_e} \quad \textbf{(3.19)}$$

Replacing (5.20) in (5.18) gives the volumetric efficiency equal with:

$$\boldsymbol{\eta_v = m \times a \times nr \times \rho_a \times V_d \times N_e} \quad \textbf{(3.20)}$$

The volumetric efficiency is maximum 1.00 (or 100%). At this value, the engine is capable of drawing all of the theoretical volume of air available into the engine. There are special cases in which the engine is specifically designed for one operating point, for which the volumetric efficiency can be slightly higher than 100 %.If intake air pressure pa [P_a] and temperature T_a [K] are measured in the intake manifold, the intake air density can be calculated as [6]:

$$\boldsymbol{\rho_a = (pa \times R_a) \times T_a} \quad \textbf{(3.21)}$$

where:

ρ_a [kg/m^3] – intake air density

p_a [P_a] – intake air pressure

T_a [K] – intake air temperature

R_a [J/kgK] – gas constant for dry air (equal to 286.9 J/kgK)

CHAPTER 4

RESULTS AND DISCUSSION

Experiments were conducted by adjusting the fuel amount with the needle valve. In this way, it is aimed to change the fuel setting continuously. The needle moving in a linearly conical housing could not be prevented from axially sliding. Parametric results could not be obtained because the fuel adjustment was irregular, but similar experiments were performed by replacing the carburetor nozzle and comparisons were made with the original Lombardini engine data. The emissions of the Lombardini engine and the HBO engine were also compared. With the needle valve, the amount of fuel was reduced, but at some point, the engine started to run irregularly. All specific fuel consumption (SFC) was high. For single cylinder engines with carburetor, it is normal that the quantities of SFC are between 300 and 400 g / hp-hour. However, electronic ignition and fuel injection improves the performance.

4.1. Test 1: Fully Open Needle Valve

The first test was done with a fully open needle valve. Table 4.1 shows the information regarding this test and the obtained results for power, torque and specific fuel consumption are represented in Figures 4.1 to 4.3. As can be seen from the figures, the obtained power was 2 HP at 1500 rpm and increased to 6 HP at 3500 rpm it. At 1500 rpm, the torque was 9 N-m, increased to 12 N-m by increasing the speed up to 3000 rpm, and with further increase of the speed to 4000 rpm, the obtained torque decreased to 10 N-m. Specific fuel consumption decreased from 370 g/hp-hour at 1500 rpm to 340 g/hp-hour at 2500 rpm then increased up to 380 at 4000 rpm.

Table 4.1: Information table of Test 1: Fully open needle valve.

Motor type :	HBO Single Cylinder
Engine cap. :	340 cc
Number of cylinders:	1
Maximum engine power:	6 HP
Maximum engine power speed:	3500 rev/min
Maximum engine torque:	12 N-m
Maximum engine torque speed:	3500 rev/min
Idle speed:	800 rev/min
Needle Valve position:	Fully Open
Date of the experiment:	11.12.2018
Experimenter :	Metin Fendal

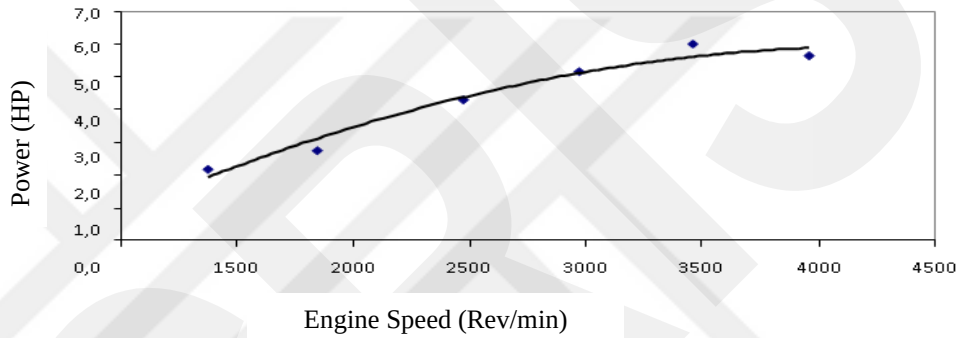

Figure 4.1: POWER-RPM relationship at fully open throttle and fully open needle valve.

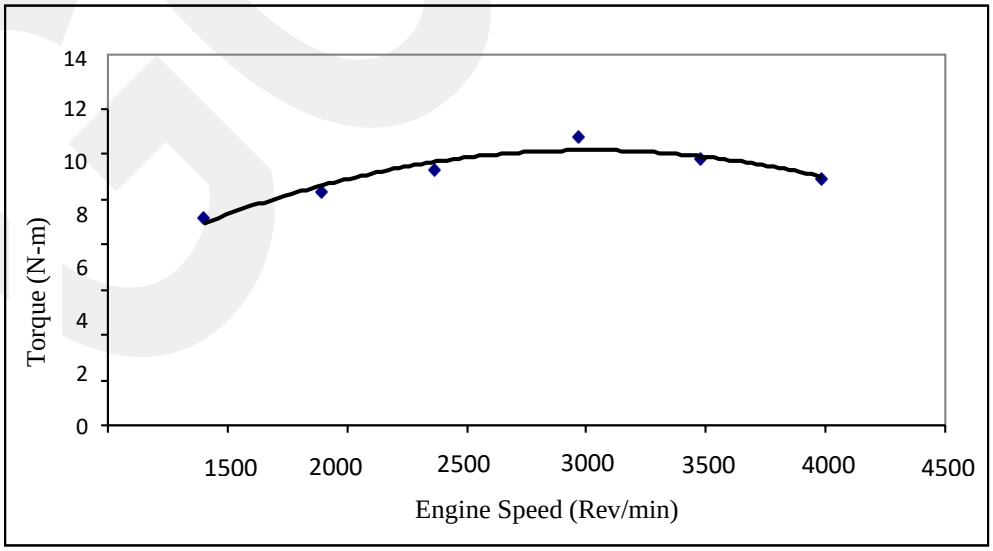

Figure 4.2: TORQUE-RPM relationship at fully open throttle and fully open needle valve.

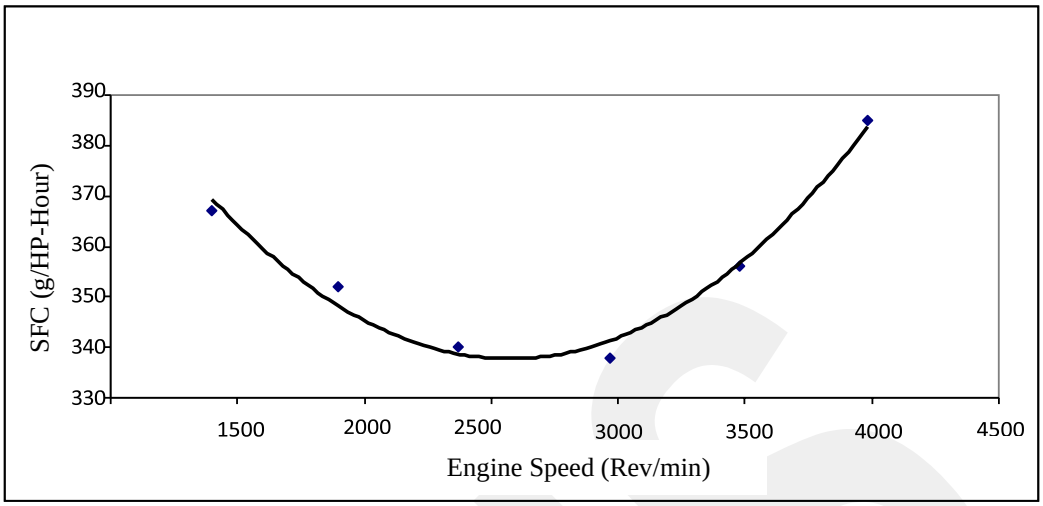

Figure 4.3: SFC-RPM relationship at fully open throttle and fully open needle valve.

4.2. Test 2: A Quarter Closed Needle Valve

The needle valve was cut down by a quarter turn according to the first state. Table 4.2 shows the information regarding this test and the obtained results for power, torque and specific fuel consumption are represented in Figures 4.4 to 4.6. Measured power values are the same as the first test. Engine torque measured maximum 14 at 2000 rpm and dropped to 12 at 4000 rpm. The reason for the increase in torque value compared to the previous experiment may be that the air fuel ratio is better in this experiment. Specific fuel values were more stable than the first test, with 350 g/hp-hour at 1500 rpm and 360 g/hp-hour at 4000 rpm.

Table 4.2: Information table of Test 2: A quarter closed needle valve.

Motor type :	HBO Single Cylinder
Engine cap. :	340 cc
Number of cylinders:	1
Maximum engine power:	6 HP
Maximum engine power speed:	4000 rev/min
Maximum engine torque:	14 N-m
Maximum engine torque speed:	2000 rev/min
Idle speed:	800 rev/min
Needle valve position:	A quarter closed
Date of the experiment:	12.12.2018
Experimenter :	Metin Fendal

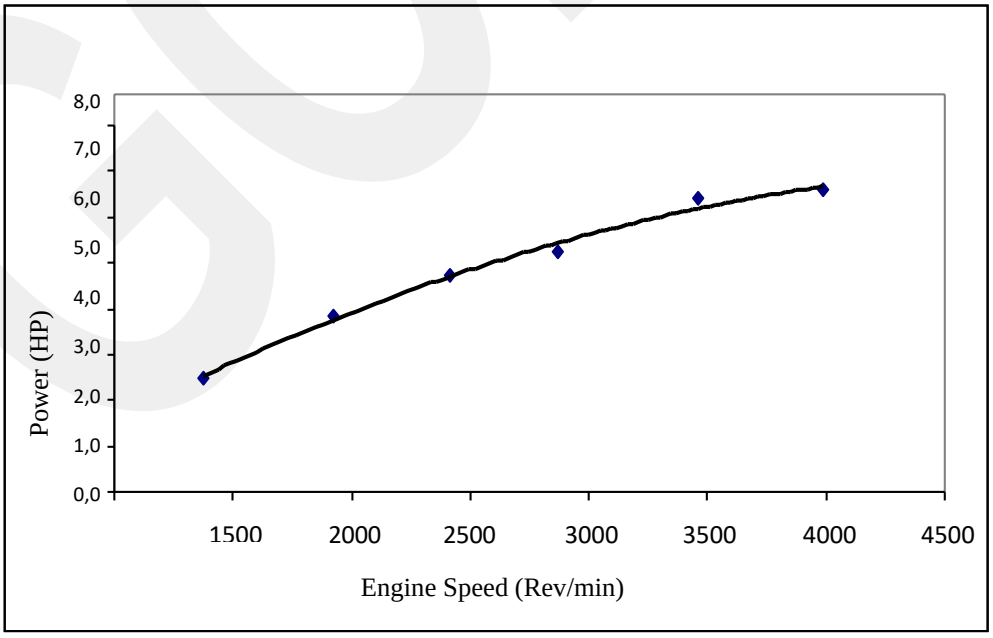

Figure 4.4: POWER-RPM relationship at full throttle and a quarter closed needle valve.

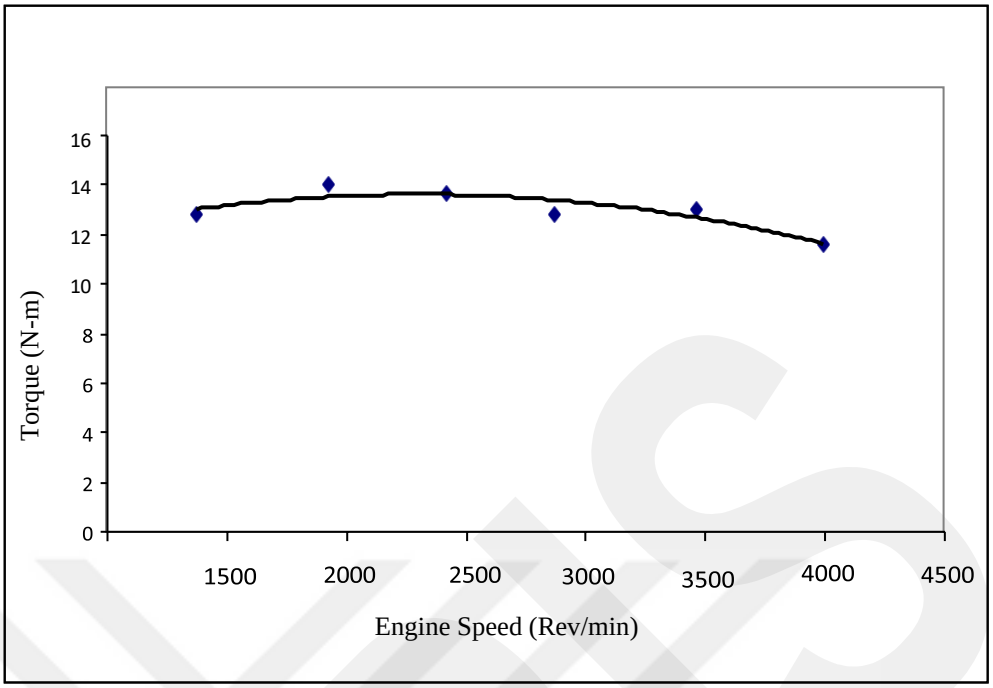

Figure 4.5: TORQUE-RPM relationship at full throttle and a quarter closed needle valve.

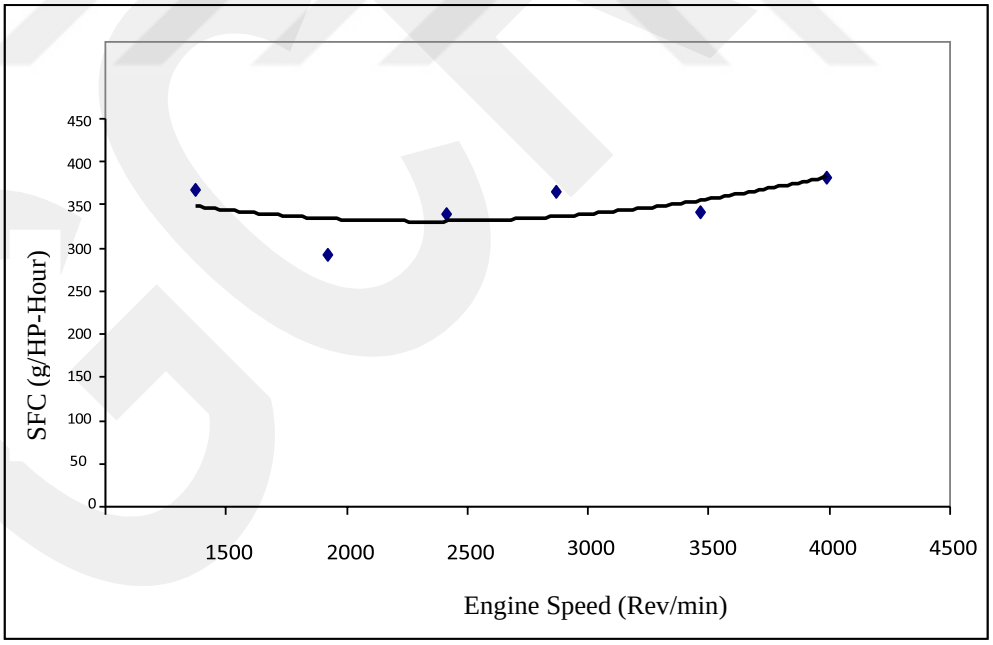

Figure 4.6: SFC-RPM relationship at full throttle and a quarter closed needle valve.

4.3. Test 3: Half Closed Needle Valve

The needle valve was cut down by a quarter turn compared to the previous test measured. Table 4.3 shows the information regarding this test and the obtained results for power, torque and specific fuel consumption are represented in Figures 4.7 to 4.9. Power values are the same as the previous test. The engine's torque values decreased compared to the previous test. Dropped from 11 N-m at 1500 rpm to 10 N-m at 4000 rpm. Highest torque value 1 N-m in 2000 rpm. Specific fuel consumption increased compared to the previous test. Increased from 380 g/hp-hour at 1500 rpm to 550 g/hp-hour at 4000 rpm.

Table 4.3: Information Table of Test 3: Half closed needle valve.

Motor type :	HBO Single Cylinder
Engine cap. :	340 cc
Number of cylinders:	1
Maximum engine power:	6 HP
Maximum engine power speed:	4000 rev/min
Maximum engine torque:	13 N-m
Maximum engine torque speed:	2000 rev/min
Idle speed:	800 rev/min
Needle valve position:	Half closed
Date of the experiment:	14.01.2019
Experimenter :	Metin Fendal

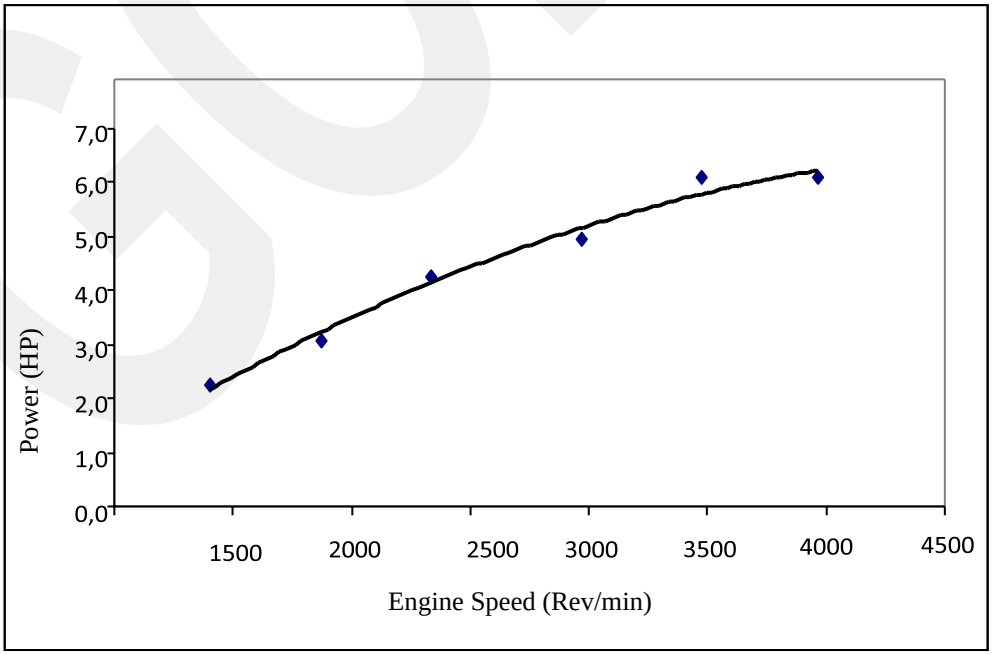

Figure 4.7: POWER-RPM relationship at full throttle and half closed needle valve.

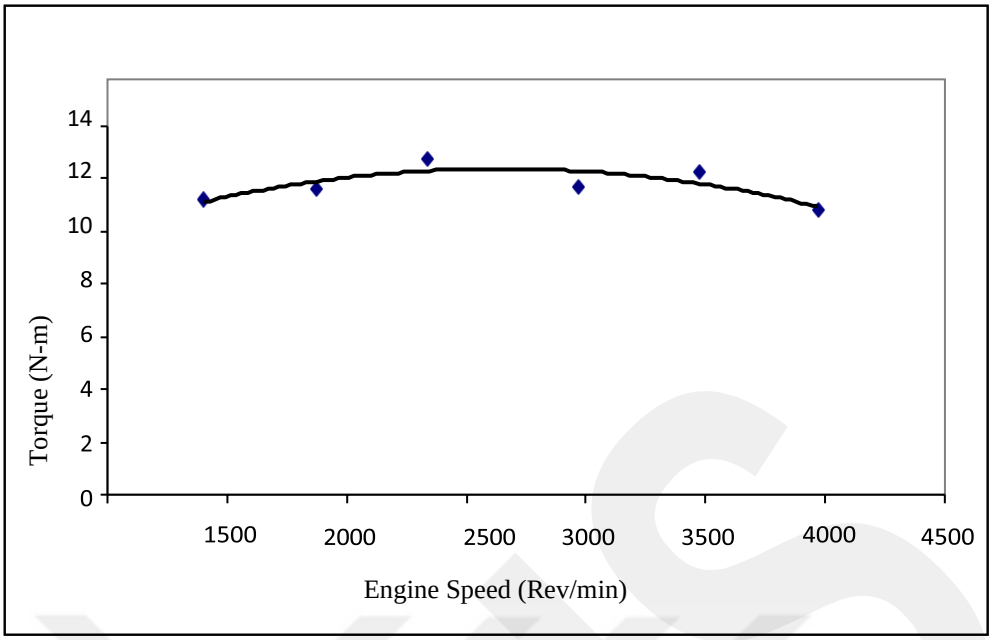

Figure 4.8: TORQUE-RPM relationship at full throttle and half closed needle valve.

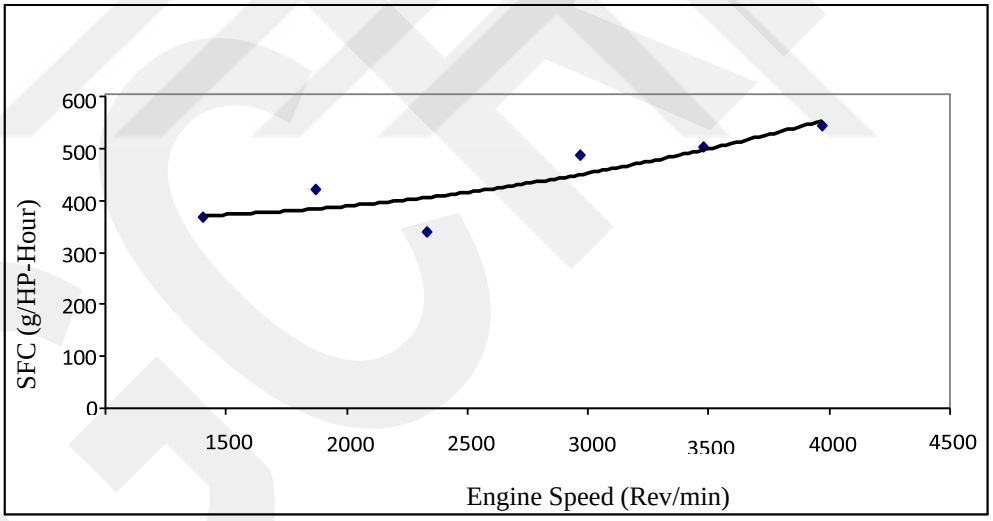

Figure 4.9: SFC-RPM relationship at full throttle and half closed needle valve.

4.4. Test 4: 3 Quarter Closed Needle Valve

The needle valve was cut down by a quarter turn compared to the previous test. Table 4.4 shows the information regarding this test and the obtained results for power, torque and specific fuel consumption are represented in Figures 4.10 to 4.12. Engine power increased from 2 horsepower at 1500 rpm to 6 horsepower at 4000 rpm. Engine torque was measured at 1500 rpm and 4000 rpm at 10 N-m, while its maximum value was measured at 12 N-m in the 2500 rpm. Specific fuel consumption increased from 400 g/hp-hour at 1500 rmp to 600 g/hp-hour at 4000 rpm. Fuel consumption increased compared to previous test.

Table 4.4: Information Table of Test 4: 3 quarter closed needle valve.

Motor type :	HBO Single Cylinder
Engine cap. :	340 cc
Number of cylinders:	1
Maximum engine power:	6 HP
Maximum engine power speed:	4000 rev/min
Maximum engine torque:	12 N-m
Maximum engine torque speed:	2500 rev/min
Idle speed:	800 rev/min
Needle valve position:	3 quarter closed
Date of the experiment:	15.01.2019
Experimenter :	Metin Fendal

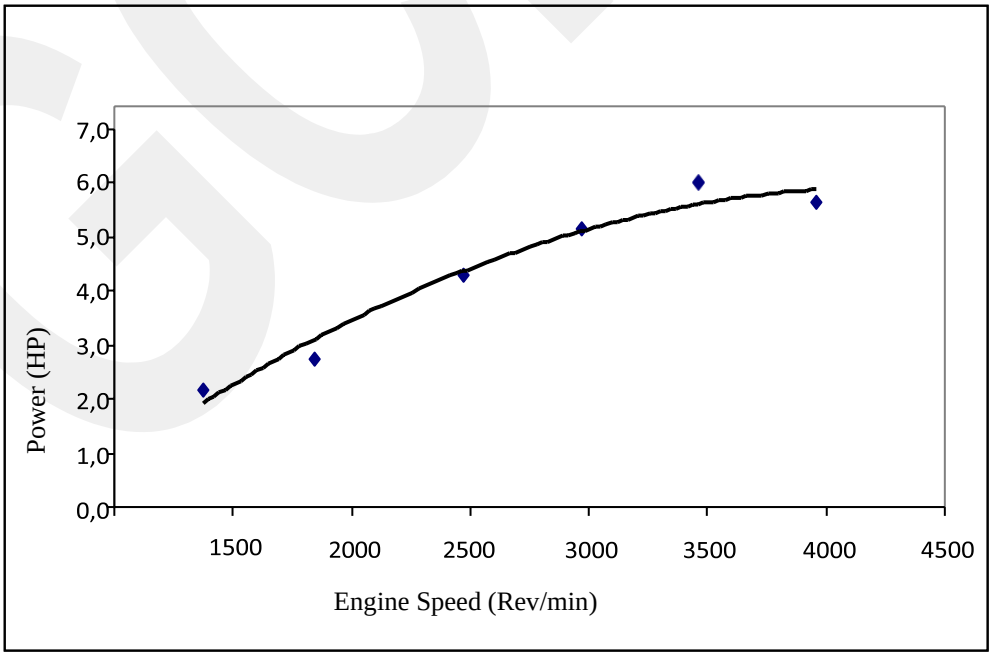

Figure 4.10: POWER-RPM relationship at full throttle and 3 quarter closed needle valve.

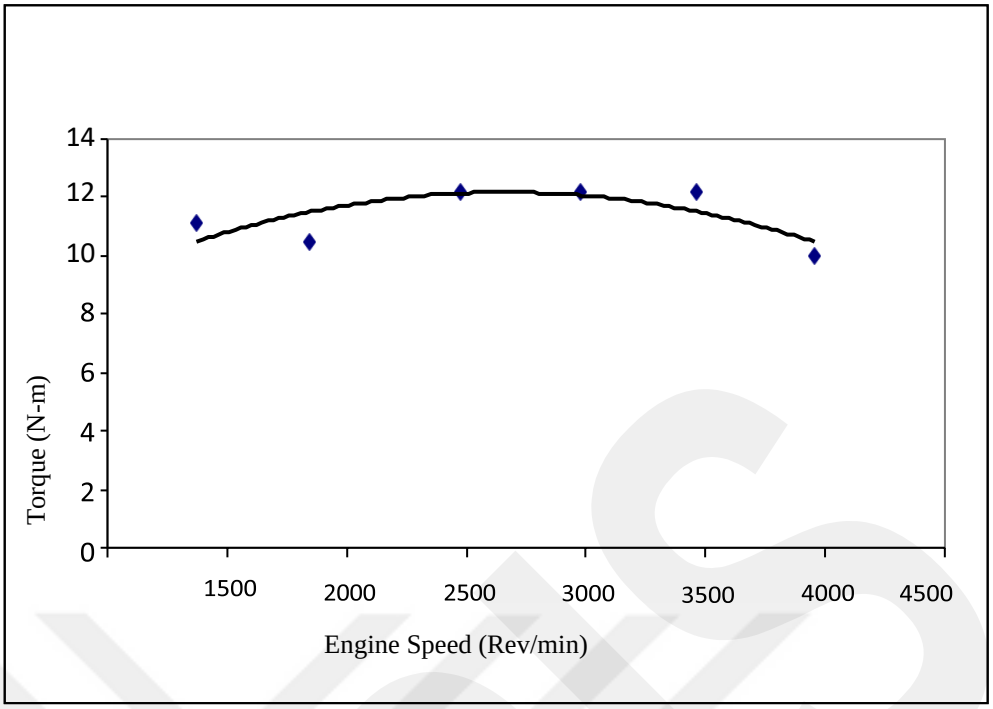

Figure 4.11: TORQUE-RPM relationship at full throttle and 3 quarter closed needle valve.

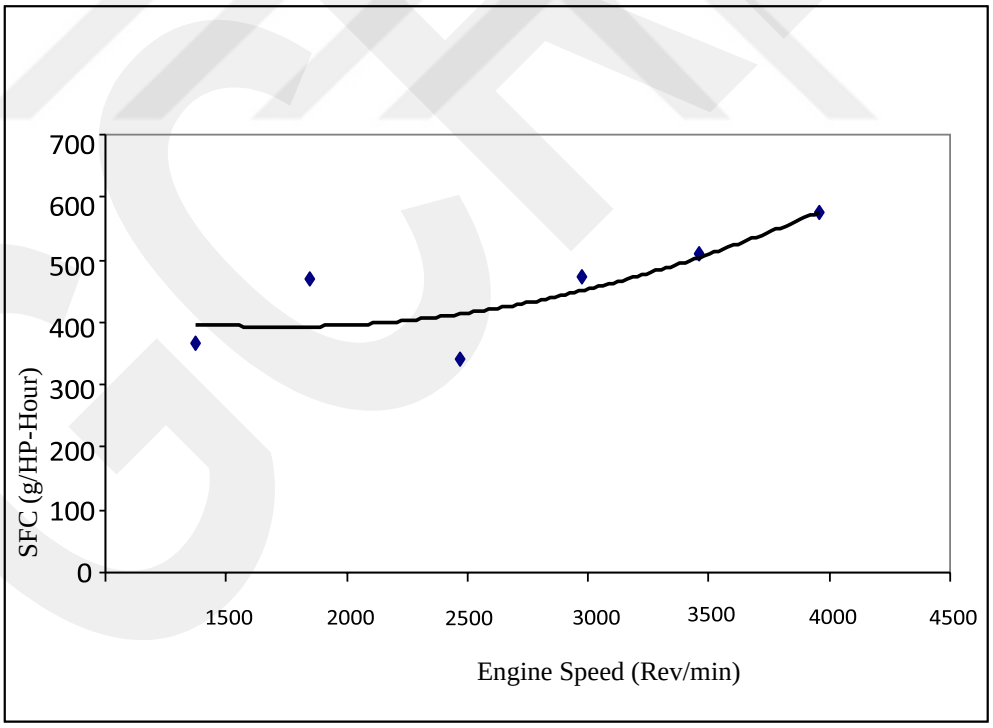

Figure 4.12: SFC-RPM relationship at full throttle and 3 quarter closed needle valve.

4.5. Test 5: A Round Closed Needle Valve

The Needle Valve Was Cut Down By A Quarter Turn Compared to The Previous Test. Table 4.5 shows the information regarding this test and the obtained results for power, torque and specific fuel consumption are represented in Figures 4.13 to 4.15. The engine power was initially measured as 2.5 horsepower at 1500 rpm and gradually increased to 9.5 N horsepower at 4000 rpm. The highest horsepower increases compared to the previous test. Engine torque increased from 13 N-m at 1500 rmp to 16 N-m at 3500 rpm. The engine torque values increased compared to previous test. Specific fuel consumption decreased from 330 g/hp-hour at 1500 rpm to 200 g/hp-hour at 4000 rpm. A large savings in specific fuel consumption was observed compared to the previous test.

Table 4.5: Information Table of Test 5: A round closed needle valve.

Motor type :	HBO Single Cylinder
Engine cap. :	340 cc
Number of cylinders:	1
Maximum engine power:	9 HP
Maximum engine power speed:	4000 rev/min
Maximum engine torque:	16 N-m
Maximum engine torque speed:	3500 rev/min
Idle speed:	800 rev/min
Needle valve position:	A round closed
Date of the experiment:	06.02.2019
Experimenter :	Metin Fendal

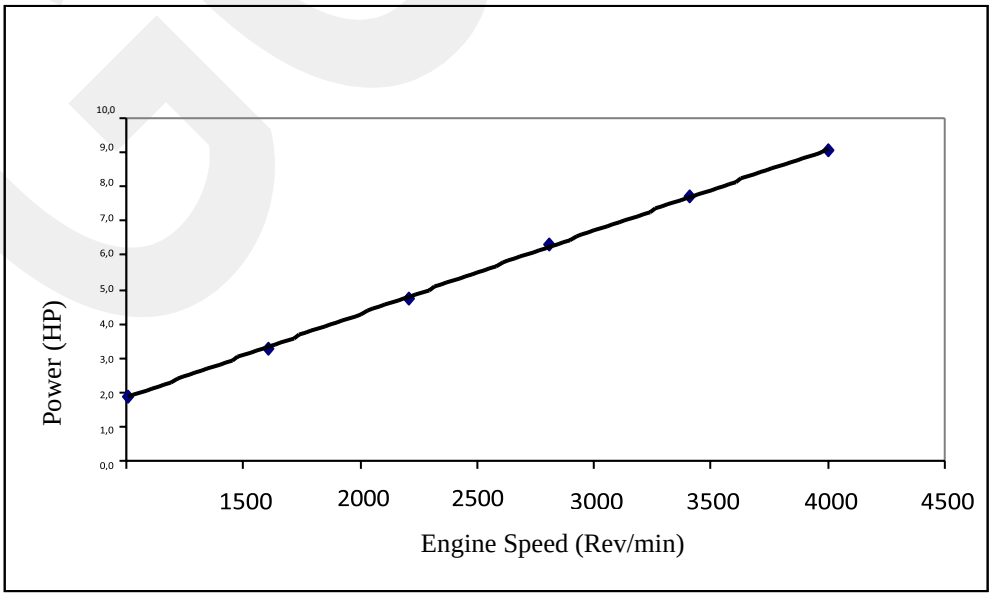

Figure 4.13: POWER-RPM relationship at full throttle and a round closed needle valve.

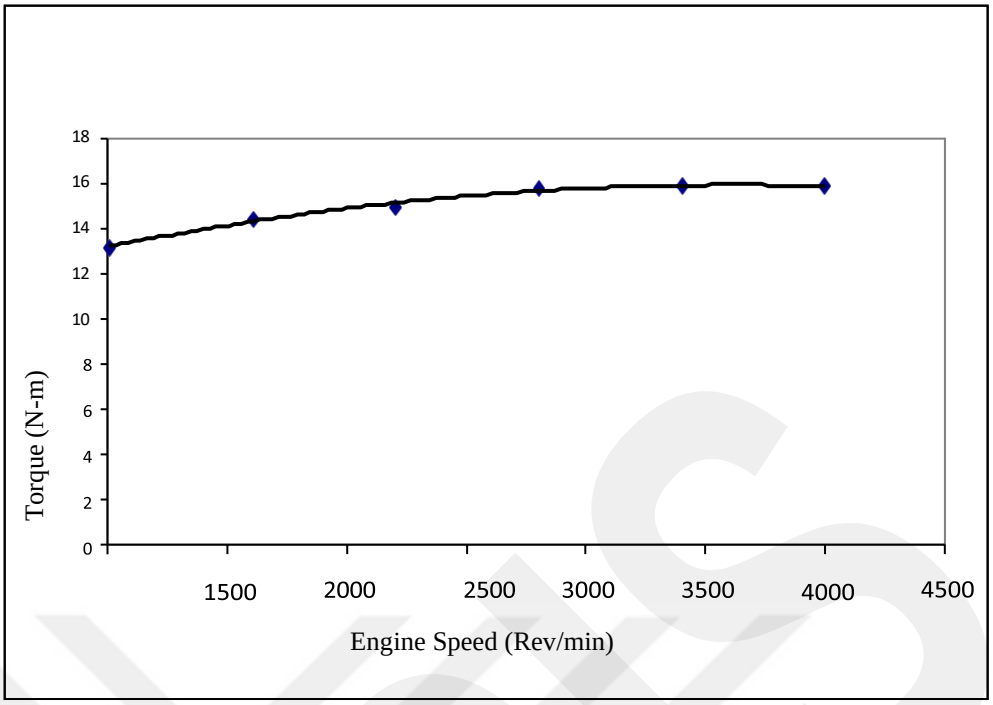

Figure 4.14: TORQUE-RPM relationship at full throttle and a round closed needle valve.

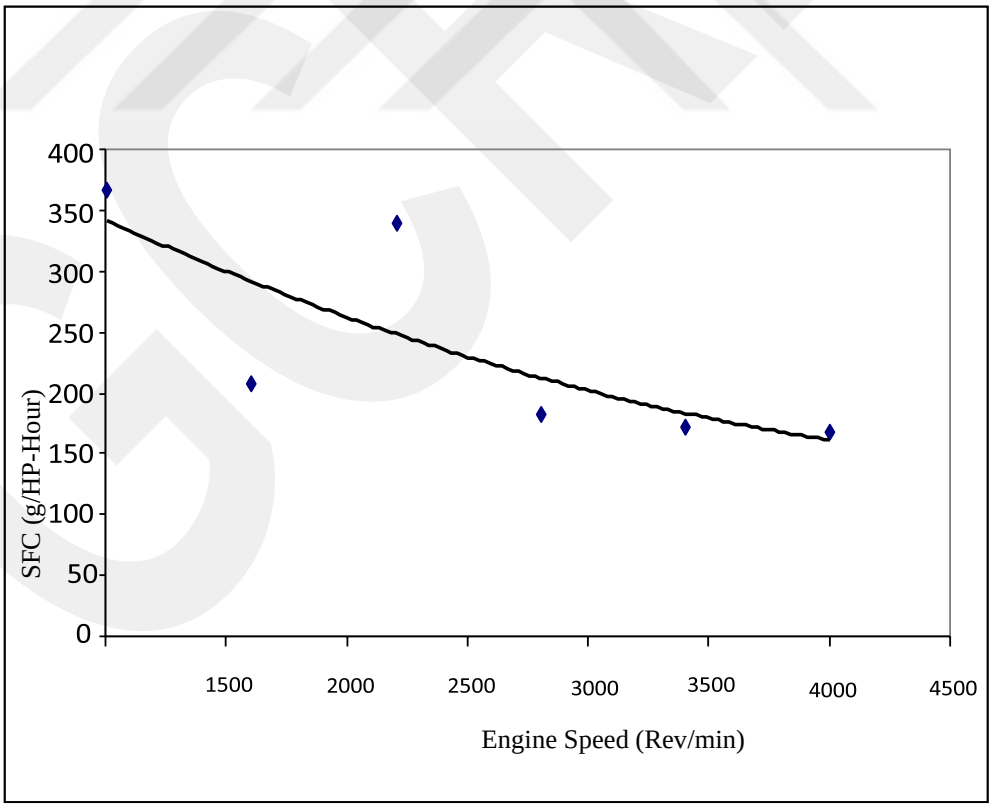

Figure 4.15: SFC-RPM relationship at full throttle and a round closed needle valve.

4.6. Test 6: Full Closed Needle Valve

The needle valve aas cut down by a quarter turn compared to the previous test. Engine power is much higher than previous tests. Table 4.6 shows the information regarding this test and the obtained results for power, torque and specific fuel consumption are represented in Figures 4.16 to 4.18. Increased from 6 horsepower at 1500 rmp to 14 horsepower at 4000 rpm. The engine's torque value, such as power, has seen its highest value in this test. Increased from 21 N-m at 1500 rpm to 25 N-m at 3500 rpm. Specific fuel consumption decreased from 330 g/hp-hour at 1500 rpm to 200 g/hp-hour at 4000 rpm.

Table 4.6: Information Table of Test 6: Full closed needle valve.

Motor type :	HBO Single Cylinder
Engine cap. :	340 cc
Number of cylinders:	1
Maximum engine power:	14 HP
Maximum engine power speed:	4000 rev/min
Maximum engine torque:	25 N-m
Maximum engine torque speed:	3500 rev/min
Idle speed:	800 rev/min
Needle valve position:	Full closed
Date of the experiment:	20.02.2019
Experimenter :	Metin Fendal

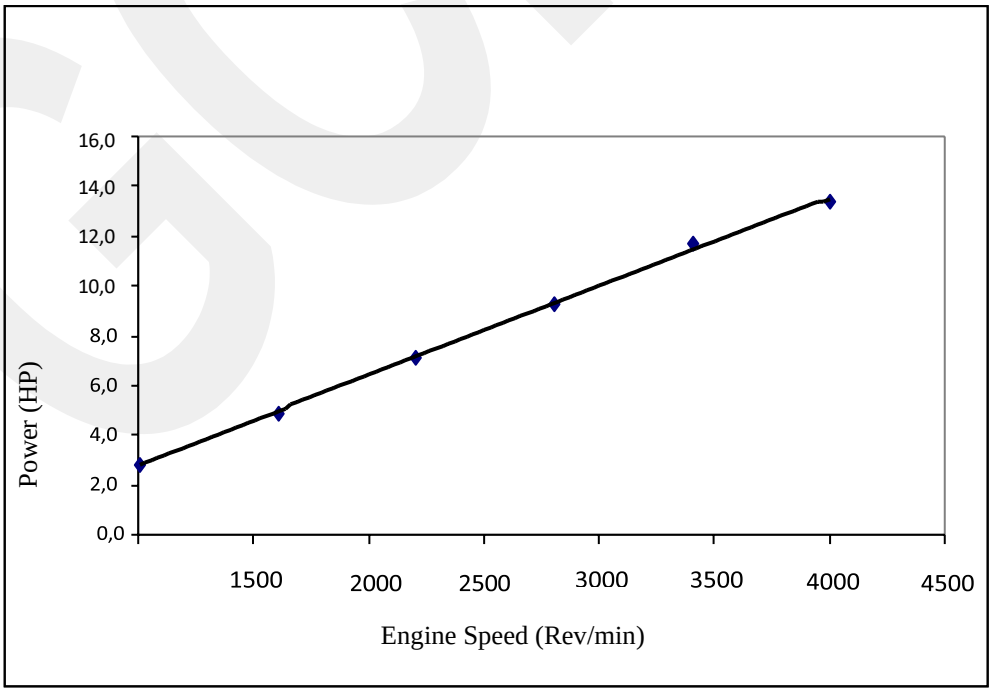

Figure 4.16: POWER-RPM relationship at full throttle and full closed needle valve.

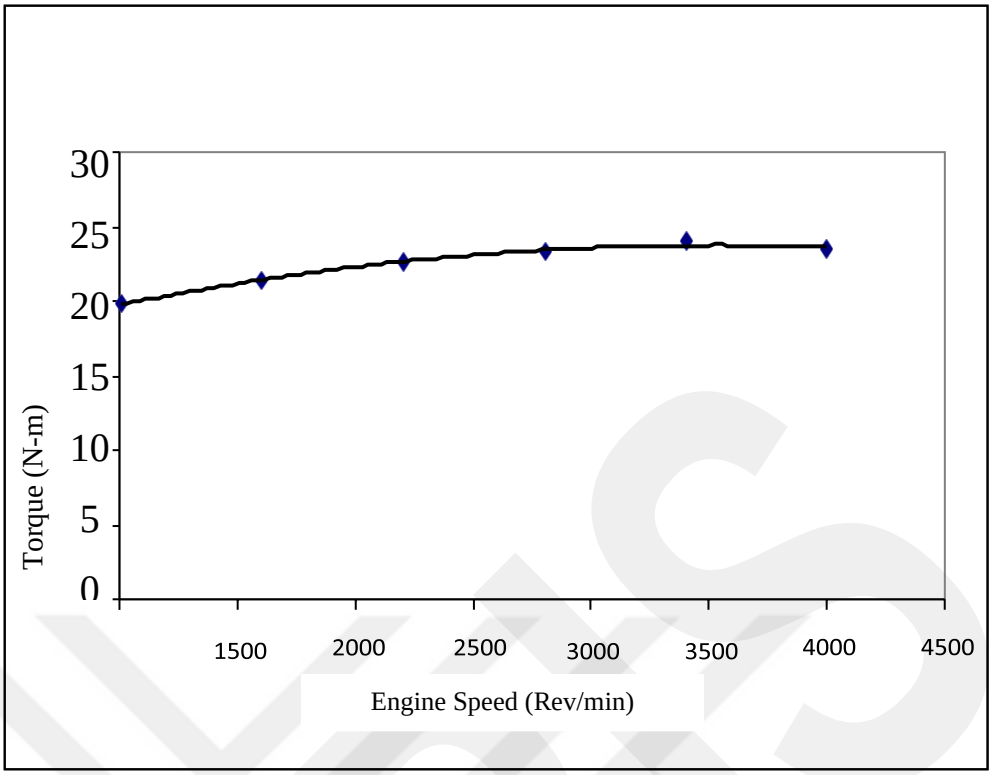

Figure 4.17: TORQUE-RPM relationship at full throttle and full closed needle valve.

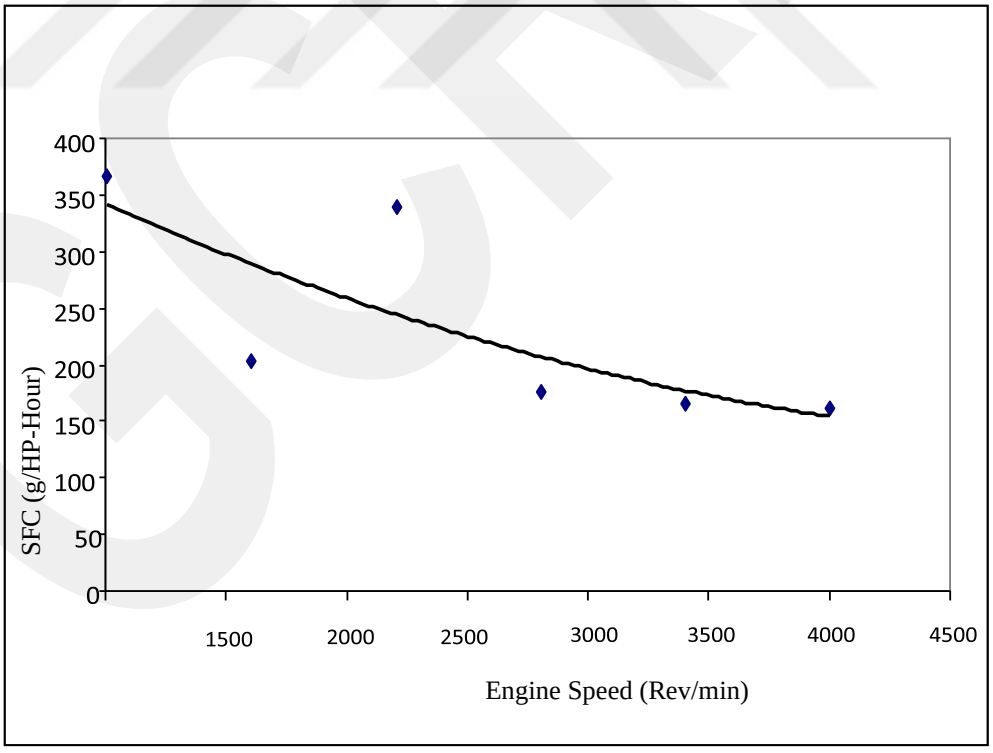

Figure 4.18: SFC-RPM relationship at full throttle and full closed needle valve.

4.7. HBO-LGA Engines Comparison

The geometry of the connecting rods of the HBO engines used in this study is different from the geometry of normal internal combustion engines. Due to this difference, the speed profile of the piston moving between the bottom dead center and the top dead center changes. When the piston speeds of the Lombardini (LGA type) single cylinder engine with the same sweeping volume as it was tried 340 cc sweeping volume engine are compared at 4000 rpm, the piston moves more slowly around the top and bottom dead centers. In the middle of its stroke, however, it moves at a higher speed for a short time in the maximum speed range of normal engines. As a result, the average speed of the piston of the HBO engine for the same crankshaft speed is lower than the average speed of the pistons of normal internal combustion engines, and the maximum crankshaft speeds of the HBO engines for the same average piston speeds may be higher. As a result of higher speed in the same engine dimensions, the power of the engine increases. Increased combustion time due to the low piston speed in the vicinity of the top dead center also extends the time required for the formation of the flame core, reducing the effect of local turbulence that will adversely affect the flame core. The velocity of the flame increases due to the lower volume increase during combustion. Due to the special structure of the connecting rod, the tangential force generated by the pressure generated in the cylinder from the start of the ignition occurs in the direction of rotation of the crankshaft, although the firing angle is before the top dead center relative to the piston [1].

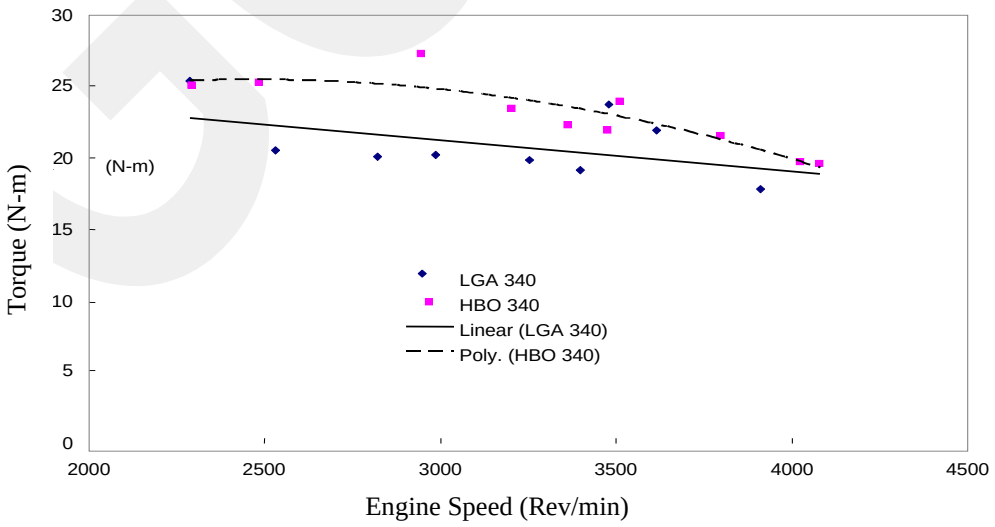

Figure 4.19: Original LGA and HBO engine torques with the same sweep volume.

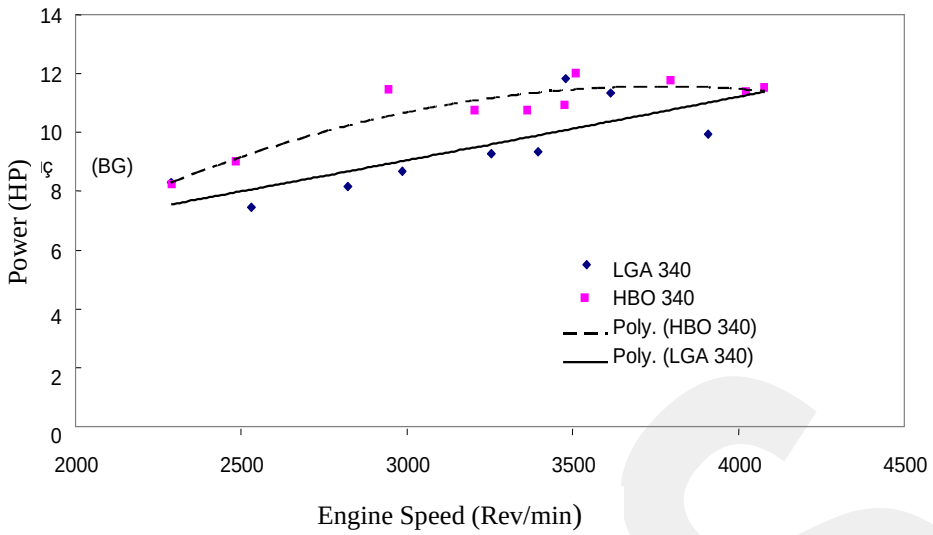

Figure 4.20: Original LGA and HBO engine powers with the same sweep volume (340 cc).

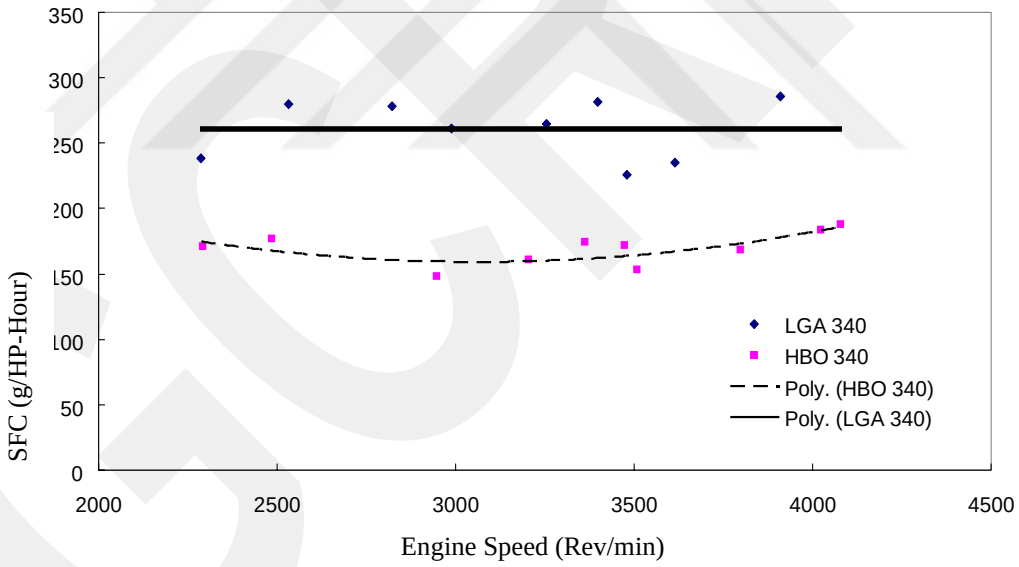

Figure 4.21: Original LGA and HBO specific fuel consumption with the same sweep volume (340 cc).

Table 4.7: LGA 340 engine test results [1].

LGA-340		1	2	3	4	5	6	7	8	9
Air inlet temperature	C	26,9	27,9	29,1	30,7	33,2	32,4	31,5	31,6	32,3
Air inlet pressure	Mbar	689	689	689	689	689	689	689	689	689
Air humidity	%	45	45	45	45	45	45	45	45	45
Engine capacity	C c	340	340	340	340	340	340	340	340	340
Engine speed	rev/min	2287	2531	3480	3614	3910	3397	2821	2987	3254
Atm. Correction Coefficient		1,121	1,125	1,130	1,136	1,146	1,143	1,139	1,140	1,142
Engine Torque	N-m	22,7	18,4	21,1	19,4	15,6	16,9	17,8	17,9	17,5
Adjusted torque	N-m	25,5	20,7	23,8	22,0	17,9	19,3	20,3	20,4	20,0
Fuel consumption	g/s	0,55	0,58	0,74	0,74	0,79	0,73	0,63	0,63	0,68
Engine power	hp	8,3	7,5	11,8	11,3	10,0	9,3	8,1	8,7	9,3
Specific fuel consumption	g/HP-hour	239	280	225	235	286	281	278	261	264

Average Specific Fuel Consumption = 261 g/hp-hr

Average Power = 9.4 hp

Average Torque= 21.1 N-m

Table 4.8: HBO 340 engine test results.

HBO-340		1		2	3	4	5	6	7	8	9	10
Air inlet temperature	C	27,8		28,6	30,1	29,8	29,8	29,7	30,2	29,5	29,1	27,8
Air inlet pressure	mbar	689		689	689	689	689	689	689	689	689	689
Air humidity	%	45		45	45	45	45	45	45	45	45	45
Engine capacity	Cc	340		340	340	340	340	340	340	340	340	340
Engine speed	rev/min	2292		2485	2946	3205	3364	3475	3510	3797	4023	4079
Atm. Correction Coefficient		1,125		1,128	1,134	1,132	1,132	1,132	1,134	1,131	1,130	1,125
Engine Torque	N-m	22,4		22,5	24,1	20,8	19,8	19,5	21,2	19,2	17,6	17,6
Adjusted torque	N-m	25,2		25,4	27,3	23,6	22,4	22,1	24,0	21,7	19,9	19,8
Fuel consumption	g/s	0,39		0,44	0,47	0,48	0,52	0,52	0,51	0,55	0,58	0,6
Engine power	hp	8,2		9,0	11,5	10,8	10,7	10,9	12,0	11,7	11,4	11,5
Specific fuel consumption	g/HP-hour	171		176	148	161	174	171	153	169	183	188

Avrg. Specific Fuel Consumption = 169 g/hp-hr

Average Power = 10.8 hp

Average Torque = 23.1 N-m

4.8. Impact of Ignition Advance on HBO Engine

Since the ignition advance in the engine used in this study can be controlled mechanically to a limited extent, the effect of approaching the ignition advance to the top dead center in the carburetor and conventional ignition experiments has limited effect on engine torque and engine power. Nevertheless, it was observed that specific fuel consumption decreased when the ignition advances increased [1].

It was possible to operate the HBO engine with a lean mixture with an air excess coefficient of 1.5. In this case, it has been found that with the change of ignition advance, engine torque, engine power and specific fuel consumption do not change much. However, the performance of the engine has increased when the ignition advance is reduced to the top dead center by electronic ignition. The effect of the air excess coefficient on the performance of the HBO engine was also investigated. It has been found that as the excess air coefficient increases, engine torque and engine power increase and specific fuel consumption decreases [1].

The compression ratio of the HBO motor used in this study was reduced to 9: 1 in order to avoid knocking. Previously used for comparison, the HBO engine with a carburetor compression ratio of 11: 1 was tried to compare under similar test conditions with a similar sweeping volume Lombardini engine, and as a result the average engine in the HBO engine in the 2000 to 4000 rev / min engine operating range torque increased from 21.1 Nm to 23.1 Nm by 9.5 percent, average engine power increased from 9.4 HP to 10.8 HP by 14.9 percent and average specific fuel consumption from 261 g / BG-hour to 169 g / BG- hours decreased by 35.2 percent [1].

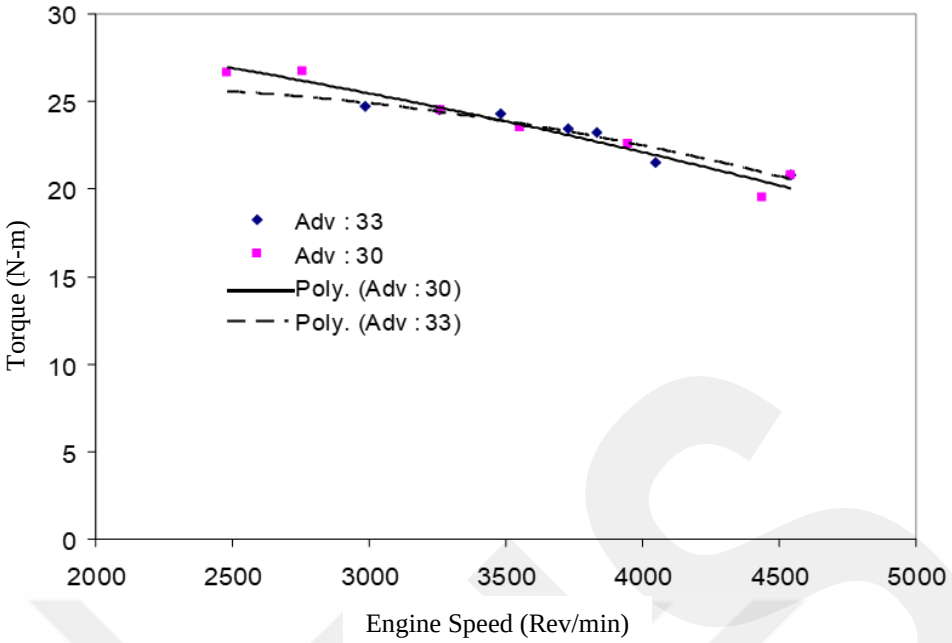

Figure 4.22: Variation of HBO engine torque with ignition advance for stoichiometric mixing.

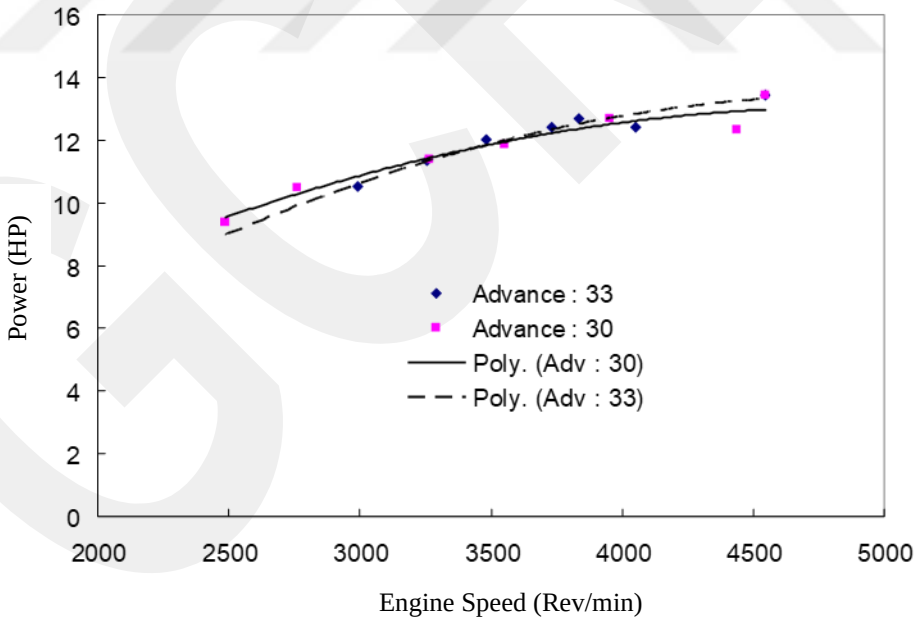

Figure 4.23: Change of HBO engine power with ignition advance for stoichiometric mixing.

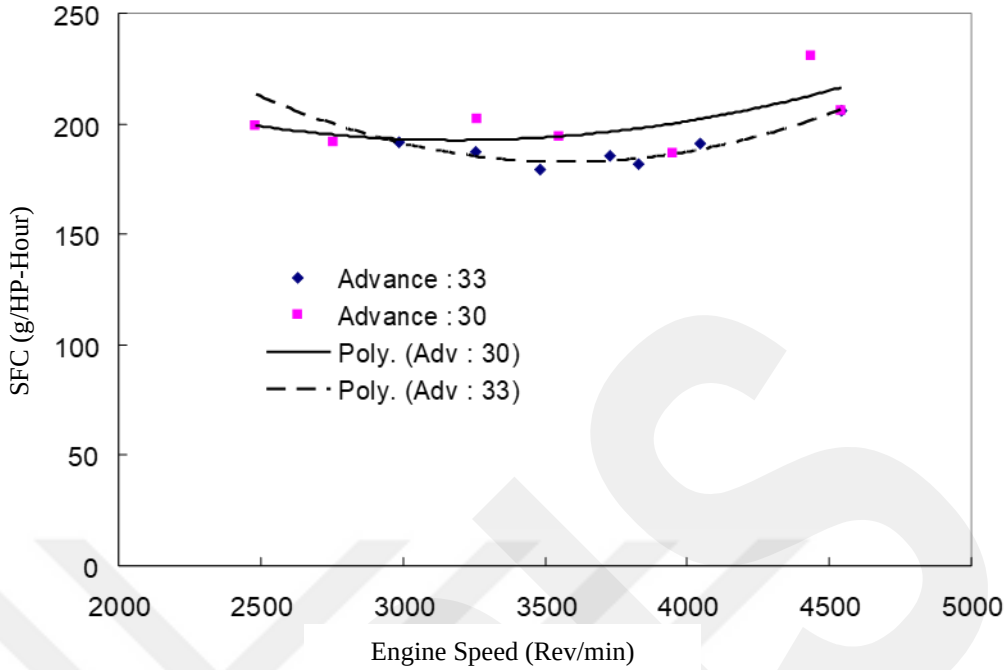

Figure 4.24: Variation of HBO specific fuel consumption for stoichiometric mixture by ignition advance.

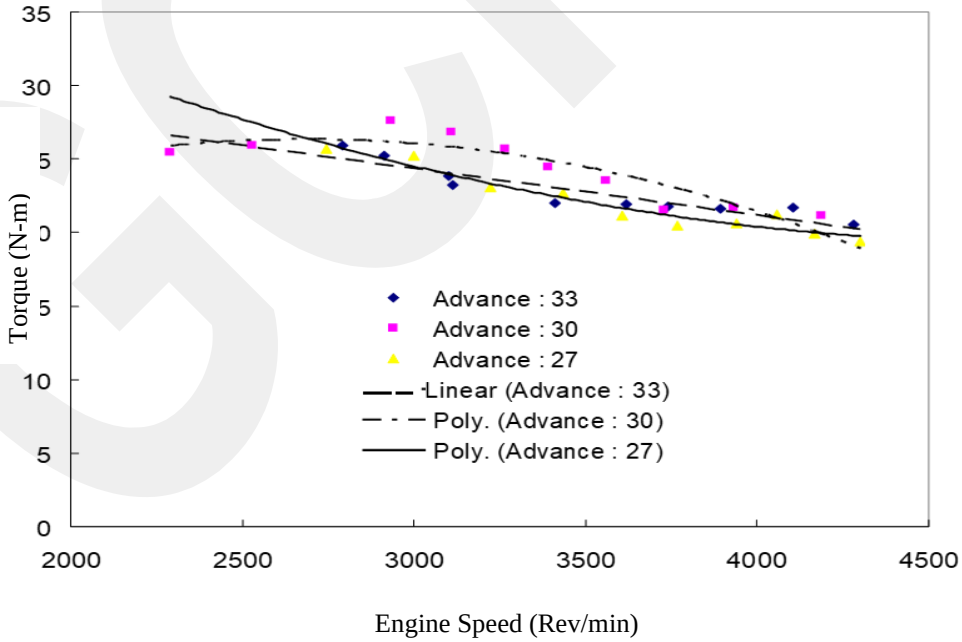

Figure 4.25: Variation of HBO engine torque with ignition advance for lean mixture.

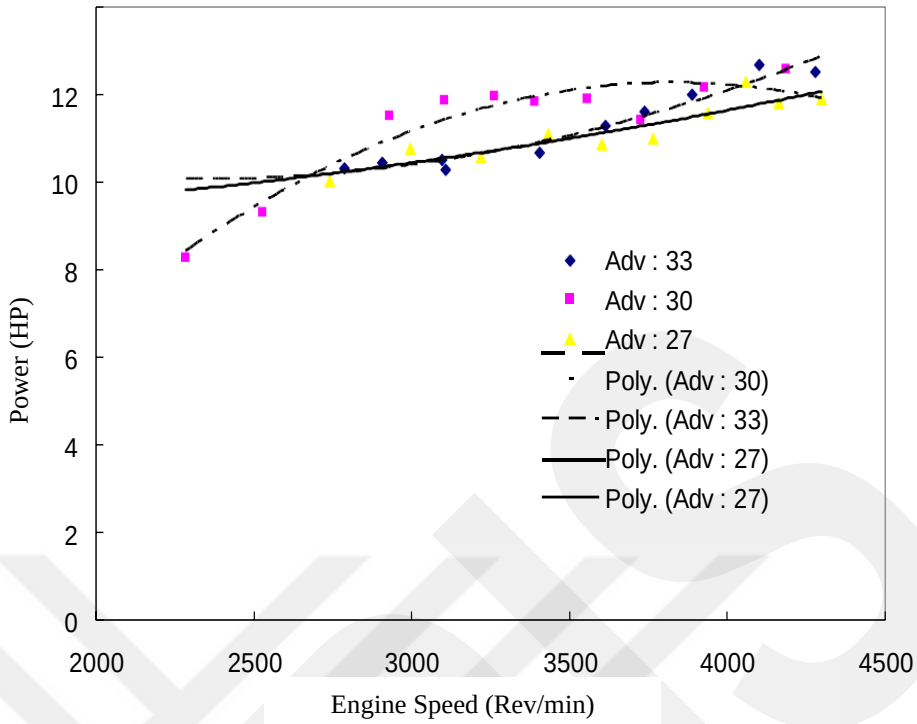

Figure 4.26: Change of HBO engine power with ignition advance for lean mixture.

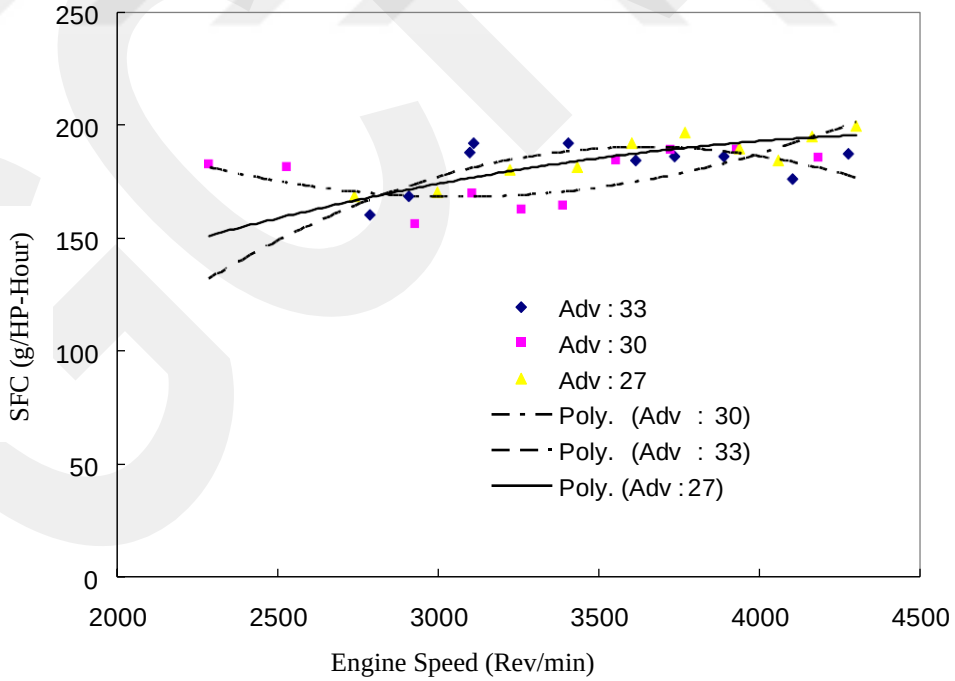

Figure 4.27: Variation of HBO consumption by ignition advance for lean mixture.

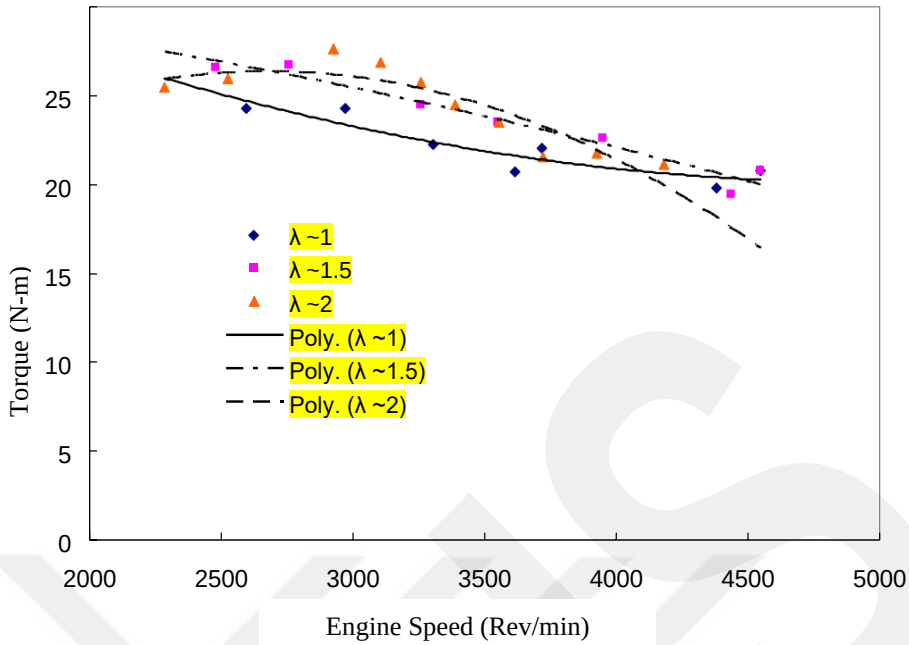

Figure 4.28: Variation of HBO engine torque with air excess coefficient.

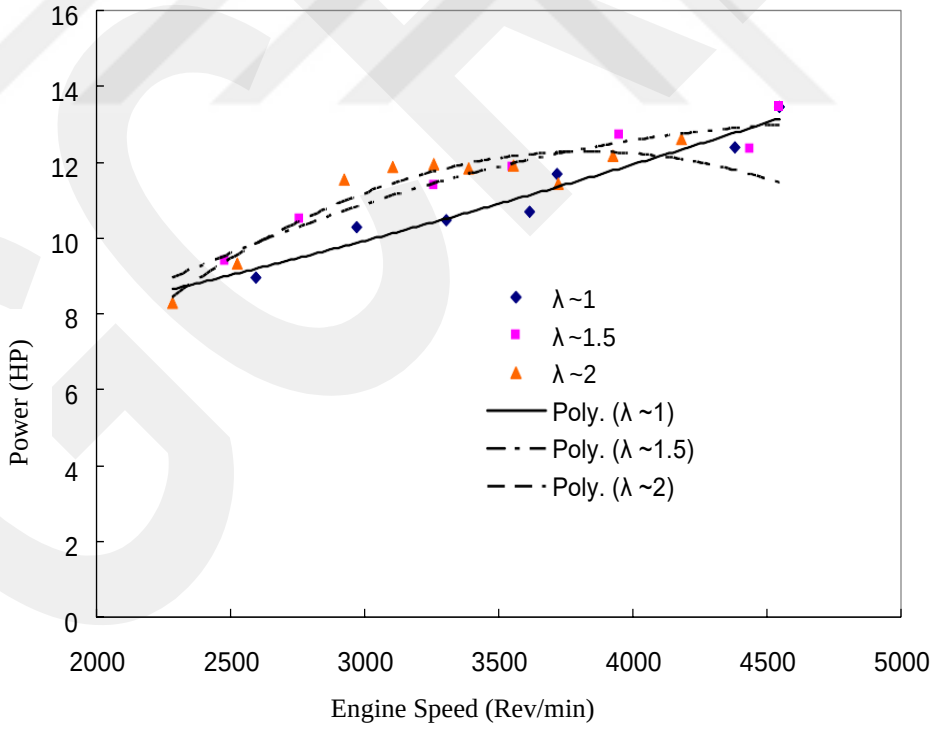

Figure 4.29: Variation of HBO engine power with air excess coefficient.

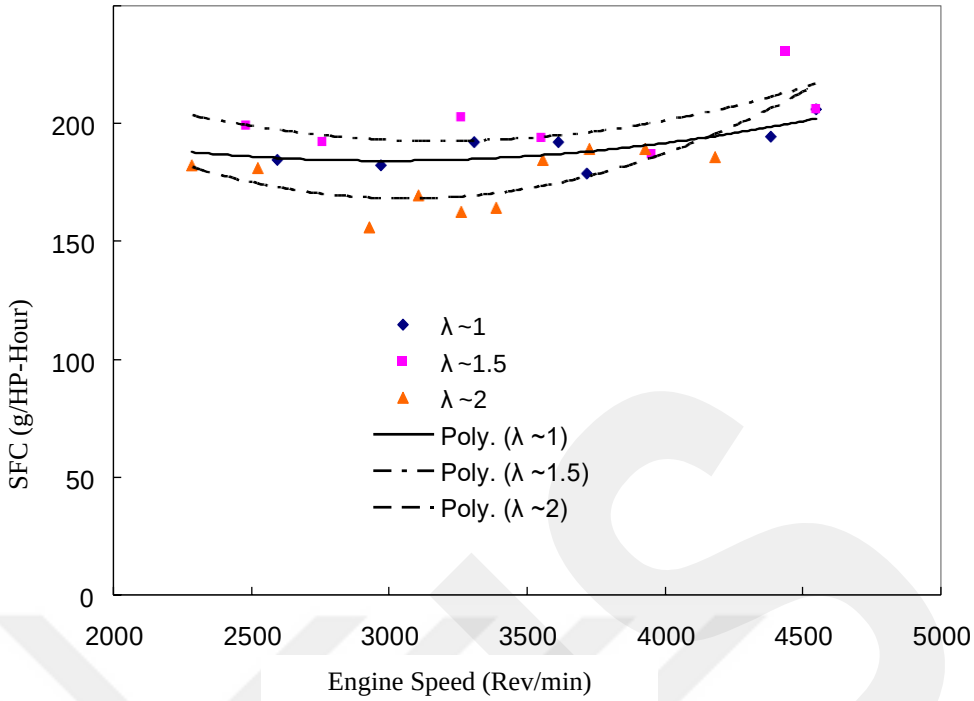

Figure 4.30: Variation of HBO specific fuel consumption with air excess coefficient.

4.9. HBO-LGA Emissions

In the emission comparison with the Lombardini engine, the reduction in carbon monoxide and unburned hydro carbon emissions show that the quality of combustion is improved. The Lombardini engine operates with a rich mixture (Lambda <1), while the HBO engine can operate with over 20 percent air surplus, which is the approximate limit for gasoline engines. This is due to the longer duration of combustion and the slow change in combustion volume.

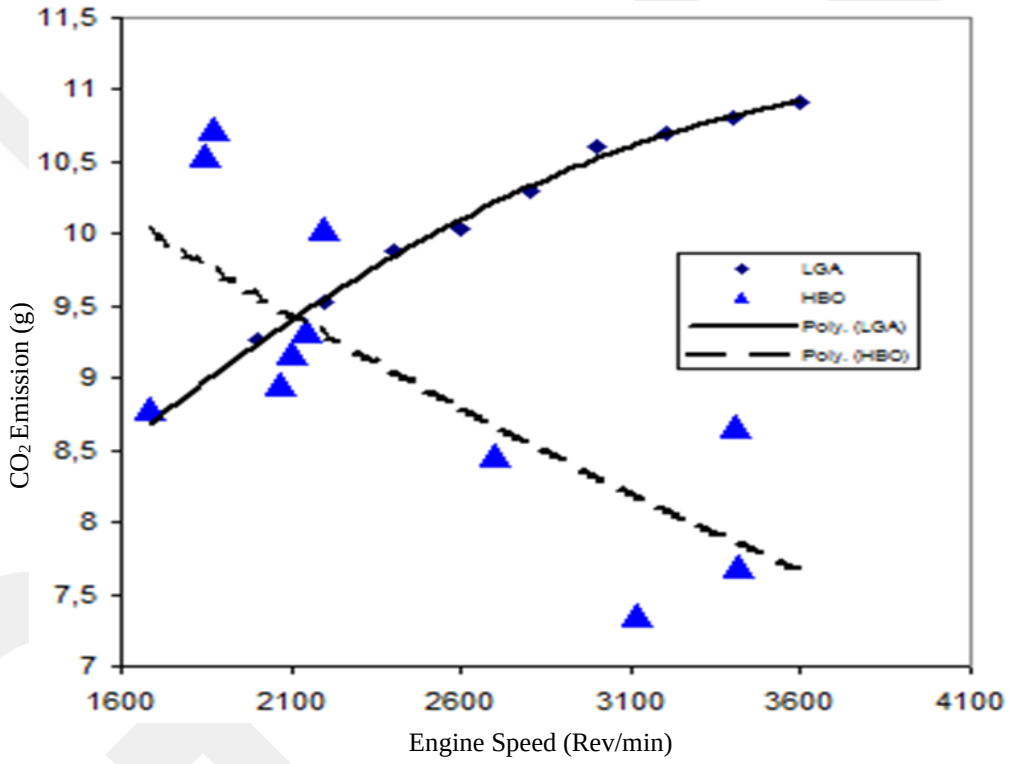

Figure 4.31: HBO – LGA carbon dioxide emissions.

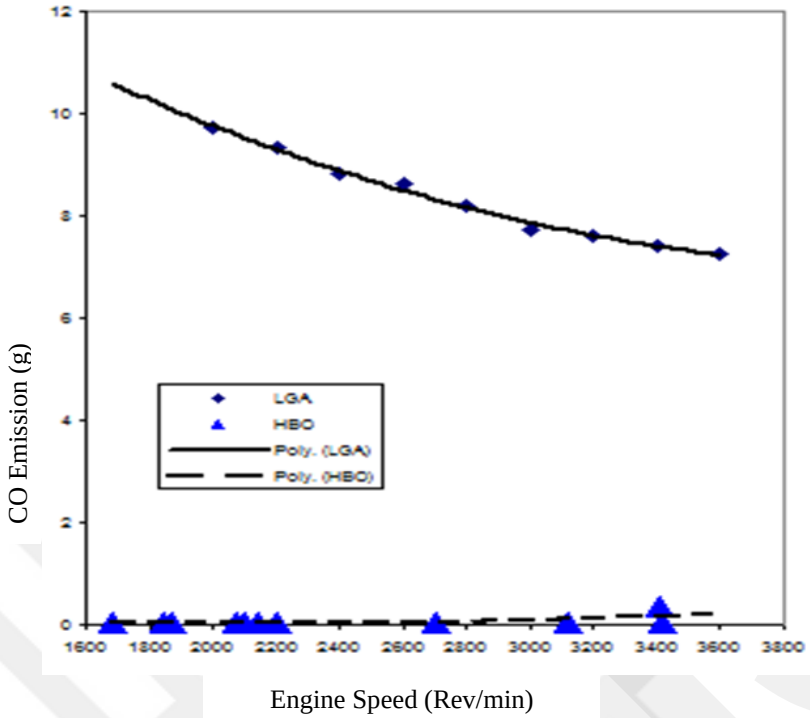

Figure 4.32: HBO – LGA carbon monoxide emissions.

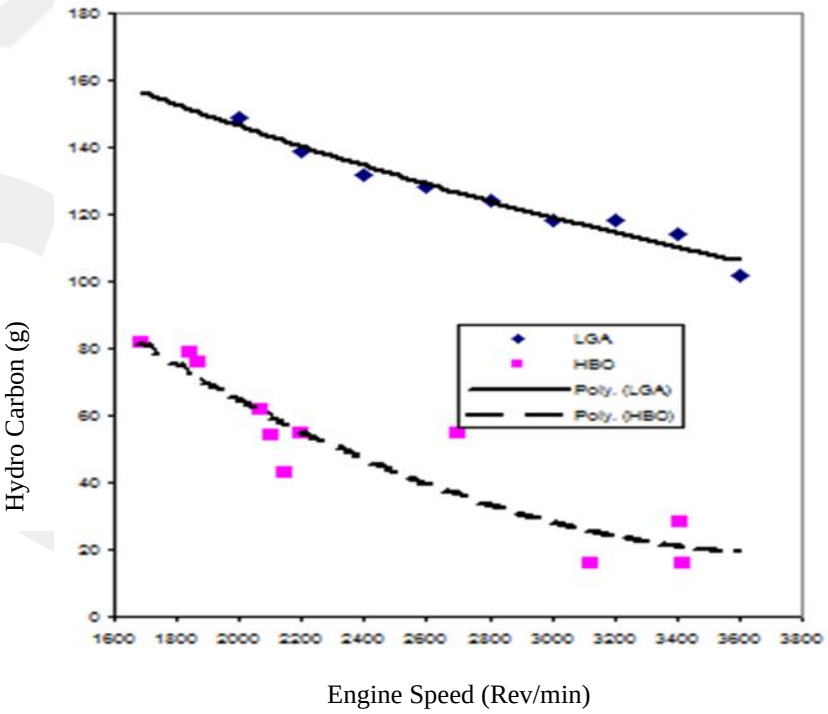

Figure 4.33: HBO – LGA hydro carbon emissions.

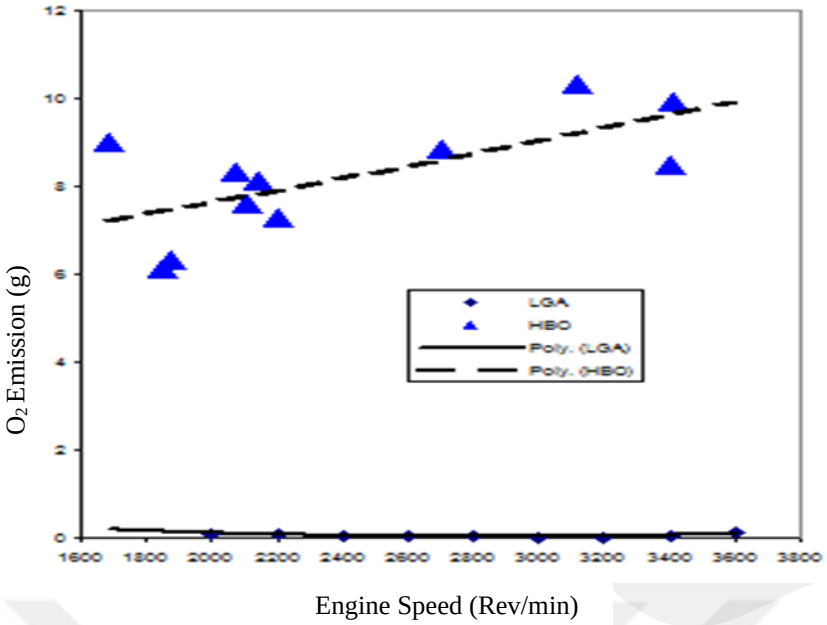

Figure 4.34: HBO – LGA oxygen emissions.

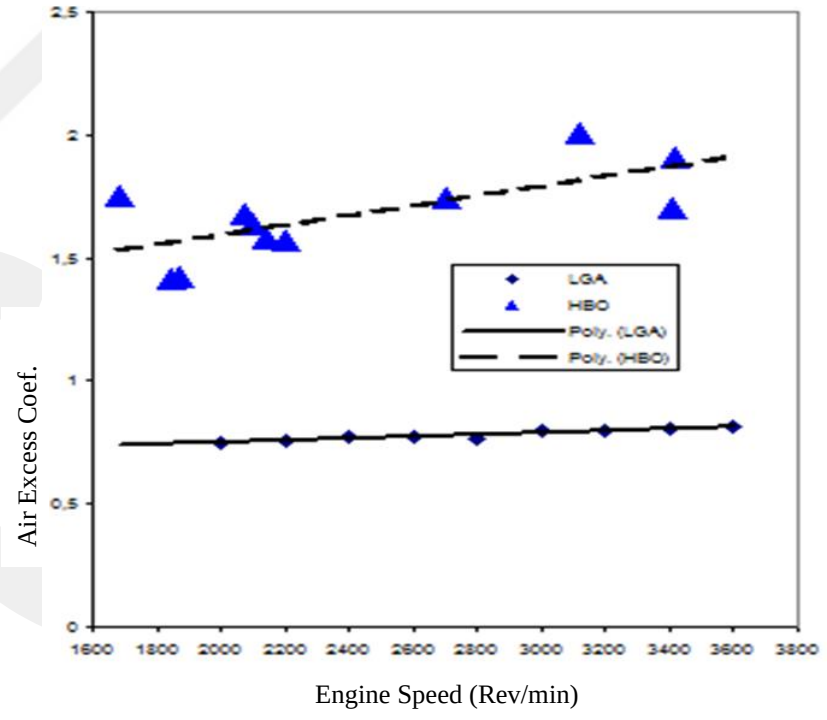

Figure 4.35: HBO – LGA air excess coefficients.

The main objective of this project was to add electronic ignition and fuel injection systems to the engines, to use these systems as they were obtained from the market

and to run and program them by providing completely empty ECU memory from the market. In this respect, the project has reached its target. Minisan has now decided to design all new prototypes with electronic ignition and fuel supply. They have found that the target was easily possible and that the cost was not high. Among its new prototypes is the 340 cc single-cylinder engine for cars.

However, the most important development achieved with this project has been the application of the ignition advance beyond the mechanically achievable ignition advance degrees in normal engines. It was thus possible to make better use of the different piston movement and speed resulting from the geometry of the crankshaft of the HBO engine. However, the valve timing and combustion chamber geometry must also be redesigned.

CHAPTER 5

CONCLUSIONS

5.1. Conclusion of The Thesis

In general, the performance of the HBO 340 engine has been observed to be better than the LGA 340 engine from which it was derived from.

- While the LGA 340 engine can run smoothly at idle without load at approximately 800 - 1000 rpm, the HBO 340 engine can run smoothly at 450 - 550 rpm. Similar performance is expected in multi-cylinder engines. Low-idle vibration-free operation is a desirable comfort element in applications such as motorcycles, fishing boats and marine boats, propeller aircraft, heavy vehicle engines.
- The lowest specific fuel consumption published by the manufacturer for the LGA 340 engine is 270 g / HP-hour, while the HBO 340 engine can operate at higher torque and power with a minimum specific fuel consumption of 153 g / HP-hour (Table 1.8). Especially in a world where unmanned aircraft, tanks and military vehicles, commercial aboveground and marine vehicles and in general oil prices are constantly increasing, all private vehicles will benefit from the fuel economy offered by HBO engine technology. The HBO engine also pollutes the environment less harmful carbon emissions by 50% (Figure 6.34) and carbon monoxide emissions by over 90% (Figure 6.33).
- The ignition advance of the HBO 340 engine approaches the top dead center according to the piston position. Thus, the maximum pressure and temperature before combustion increases and the negative work against the rising piston is reduced or even eliminated. With the improvement of the combustion chamber, spark plug layout, valve timing, intake port and manifold design, negative work against the rising piston can be completely eliminated. Engines with HBO engine technology will have new combustion chamber designs suitable for constant volume combustion. In both gasoline and diesel engines, new types of fuels suitable for the new combustion model will be produced.
- Improved intake and exhaust valve timing of the HBO 340 engine; a) the suction

valve may be provided to remain open longer than the bottom dead center in terms of the crank angle; b) the opening of the exhaust valve near the bottom dead center (even at the bottom dead center) will benefit more from the positive work of the expanded gases. New variable valve timing strategies will be created for the engines where HBO engine technology is applied.

- The new combustion chamber and piston designs of the HBO engine, which will remain around the top dead center even though the crank angle normally moves, will be able to produce ultra-low-mixture, efficient, ultra-low emission models with a low-impact, constant-volume combustion. New sensors will be added to the electronic control units for motors with HBO motor technology. Boundary knocking combustion models will be studied and the movements of ultra-lean mixtures in the combustion chamber will be examined in depth.
- HBO engine modification is achieved by replacing the basic parameters of the LGA 340 engine with parts that can be manufactured with existing technology without adding new mechanisms with geometric arrangement.

CHAPTER 6

FUTURE WORK

1. In this study, original camshaft is used in HBO motors. Parametric operation will be required using three or four separate camshafts with suction and exhaust cams arranged at different angles.
2. In spite of all its advantages, optimization of the above-mentioned parameters will be required in order to achieve high specific power, low specific fuel consumption and low specific harmful emission targets in HBO engines systems should be developed. In this study, the design changes required for electronic ignition and electronic fuel injection of single and multi-cylinder HBO engines have been successfully implemented.
3. The engine body, which is also manufactured modularly, can be completely machining and aluminum. Cooling channels can be designed and manufactured precisely. With its modular structure, it can easily work under heavy load as a twelve-cylinder boxer type engine.

REFERENCES

[1] A.D. Bayka, M. Fendal, "Özgün HBO İçten Yanmalı Motor Geliştirilmesi", TÜBİTAK Proje No: 115M079, Mart 2019.

[2] H.B. Ozdamar, "H.B.O. ENGINE", International Publication Number: WO 2010/030254 A1, 18 March 2010.

[3] LOMBARDINI LGA-340 OHC Series Work Shop Manuel, Code: 1-5302-528, 31 January 2001.

[4] S. Ratiu, "The History Of The International Combustion Engine," University Politehnica Timişaora Faculty Of Engineering Hunedoara, 2003.

[5] H. Aydoğan, M. Acaroğlu, 2009. "Günümüz İçten Yanmalı Motorlarında Kullanılan Kontrol ve Veri İletim Sistemleri ve Gelişmeler", Taşıt Teknolojileri Elektronik Dergisi (TATED), Cilt: 1, No: 2, (51-62).

[6] S. Sağıroğlu, 2006 "Buji İle Ateşlemeli Bir Motorda Elektromanyetik Kumandalı Supap Mekanizması Tasarımı, İmalatı Ve Uygulanabilirliğinin Araştırılması" Gazi Üniversitesi Fen Bilimleri Enstitüsü, Doktora tezi.

[7] M.M. Schechter, M.B. Levin, 1996. "Camless Engine", Ford Research Lab. SAE Transactions Journal of Engines, 960581, 105 (3): 622-635.

[8] A.D. Bayka, İ.H. Bayka, B. Erbil," Karşılıklı Pistonlu Eksenel Kamlı İçten Yanmalı Motor" , Türk Patent Enstitüsü, Patenti No: TR 2004 01655 Y.

[9] J.B. Heywood, 1988. "Internal Combustion Engine Fundamentals", McGraw-Hill Book Company, 248-270, 869-874.

[10] L. Eriksson, 2007. "Modeling and Control of Turbocharged SI and DI Engines", Oil &Gas Science and Technology – Rev. IFP, 62, 4, 523-538.

[11] P. Moulin, J.Chauvin, 2011. "Modeling And Control Of The Air System Of A Turbocharged Gasoline Engine" Control Engineering Practice19, 287–297.

[12] C. Voser vd., 2012. "In Cylinder Boosting of Turbocharged Spark-Ignited Engines", Part 1:Model Based Design Of The Charge Valve, Proc. Inst. Mech. Eng. Part D J. Automob. Eng., 226, 1408-1418.

[13] P. Zsiga, "Configurable Hydraulic System," 2013.

[14] T.Manganello, 2008. "BorgWarner Predicts Rapid Growth İn GDI Engines", Automotive Engineer, November 2008, 5.

[15) F. Zhao vd, 1999. "Automotive Spark-İgnited Direct-İnjection Gasoline Engines", Progress in Energy and Combustion Science, 25 1999, 437–562.

[16] Y. Takagi, 1996. “The Role of Mixture Formation in Improving Fuel Economy and Reducing Emissions of Automotive S.I. Engines. FISITA Technical Paper, No. P0109.

[17] M. Alperstein vd, 1974. “Texaco’s Stratified Charge Engine—Multifuel, Efficient, Clean, And Practical”, SAE Technical Paper, No. 740563.

[18] A.J. Scussei vd, 1978 “The Ford PROCO Engine Update”, SAE Technical Paper, No. 780699. [16] Kume T., vd, 1996. “Combustion Control Technologies For Direct İnjection SI Engine”, SAE Technical Paper, No. 960600.

[19] H. Ando vd, 1998. “Combustion Control For Mitsubishi GDI Engine”, Proceedings Of The Second International Workshop On Advanced Spray Combustion, Hiroshima, Japan, 24–26 November, Paper No. IWASC9820, 225–35.

[20] J. Yang, R. Anderson, 1998. “Use Of Split Fuel İnjection To İncrease Full-Load Torque Output Of A Direct-İnjection SI Engine”, SAE Technical Paper, No. 980495.

[21] R. Mehdiyev vd, 2003. “Benzin Motorlarında İki aşamalı Yanma Mekanizması”, I. Ege Enerji Sempozyumu ve Sergisi, Denizli, Mayıs 2003.

[22] P.G. Aleiferis vd, 2004. “The Nature Of Early Flame Development İn A Lean-Burn Stratified-Charge Spark-İgnition Engine”, Combustion And Flame 136, 283–302.

[23] Y. Sekmen, P. Sekmen, ve M.S. Salman, 2007. “Buji Ateşlemel Mir Motorun Sıkıştırma Oranı Değişiminin Motor Performansı ve Egzoz Emisyonlarına Etkisi”, Gazi Üniv. Müh. Mim. Fak. Der. Cilt 22, No 4, 745-751.

[24] A. Akbaş, Y. Sekmen ve P. Erduranlı, 2003. “Sıkıştırma Oranı Artışının LPG ile Çalışan Buji ile Ateşlemeli Taşıt Motorunun Gücü ve Yakıt Ekonomisine Etkisi”, Makina Tasarım ve İmalat Dergisi, Cilt:5, No.1, 29-34.

[25] D.L. Boggs, H.S. Hilbert, 1995. “The Otto-Atkinson Cycle Engine Fuel Economy and Emissions Results and Hardware Design”, SAE, Paper No: 950089.

[26] S. Muranaka, Y. Takagi, T. Ishida, 1987. “Factors. Limiting The Improvement in Thermal Efficiency of Spark Ignition Engine at Higher Compression Ratio”, SAE, Paper No: 870548, 1-11.

[27] G.H. Abd Alla, 2002. “Computer Simulation of A Four-Stroke Spark Ignition Engine”, Energy Conversion&Management, 43, 1043-1061.

[28] J.A.A. Yamin, and M.H. Dado, 2004. “Performance simulation of a four-stroke engine with variable stroke-length and compression ratio”, Applied Energy, 77(4), 447-463.

[29] N.N. Mustafi, Y.C. Miraglia, R.R. Raine, P.K. Bansal, and S.T. Elder, 2006. “Spark-ignition Engine Performance with ‘Powergas’ Fuel (mixture of CO/H2): A Comparison with Gasoline and Natural Gas”, Fuel, 85 (12-13), 1605-1612.

[30] J.A.A.Yamin, H.N. Gupta, B.B. Bansal and O.N. Srivastava, 2000. “Effect of Combustion Duration on The Performance and Emission Characteristics of a Spark Ignition Engine Using Hydrogen As a Fuel”, International Journal of Hydrogen Energy, 25(6), 581-589.

[31] M.B. Çelik, M.K. Balki, 2007. “Düşük Güçlü Bir Motora Farklı Sıkıştırma Oranlarında LPG Kullanımının Performans ve Emisyonlara Etkisi”, Gazi Üniv. Müh. Mim. Fak. Der. Cilt 22, No 1, 81-86.

[32] W.H. Adams, H.G. Hinrichs, P. Adamis, 1987. “Analysis of The Combustion Process of A Spark Ignition Engine with A Variable Compression Ratio”, SAE, Paper No: 870610.

[33] R. Mehdiyev, D. Bayka, H. Arslan, ve T. Güdü, 2005. “Düşük Emisyonlu ve Yüksek Verimli Yeni Bir Kademeli Dolgulu Benzin Motoru“, Mühendis ve Makina, Cilt 46, Sayı 549, Sayfa 42-50.

[34] B.L. Salvi, K.A. Subramanian, 2014 “Experimental İnvestigation And Phenomenological Model Development Of Flame Kernel Growth Rate İn A Gasoline Fuelled Spark İgnition Engine” Applied Energy 139, 93–103.

[35] E. Corti, vd., 2014 “Transient Spark Advance Calibration Approach”, Energy Procedia 45, 967 – 976.

[36] G. G. Zhu, vd, 2007. “Closed-Loop Ignition Timing Control for SI Engines Using Ionization Current Feedback”, IEEE Transactions On Control Systems Technology, 15.